

REPORT ITU-R M.2135

**Guidelines for evaluation of radio interface technologies
for IMT-Advanced**

(2008)

1 Introduction

International Mobile Telecommunications-Advanced (IMT-Advanced) systems are mobile systems that include the new capabilities of IMT that go beyond those of IMT-2000. Such systems provide access to a wide range of telecommunication services including advanced mobile services, supported by mobile and fixed networks, which are increasingly packet-based.

IMT-Advanced systems support low to high mobility applications and a wide range of data rates in accordance with user and service demands in multiple user environments. IMT-Advanced also has capabilities for high-quality multimedia applications within a wide range of services and platforms providing a significant improvement in performance and quality of service.

The key features of IMT-Advanced are:

- a high degree of commonality of functionality worldwide while retaining the flexibility to support a wide range of services and applications in a cost efficient manner;
- compatibility of services within IMT and with fixed networks;
- capability of interworking with other radio access systems;
- high-quality mobile services;
- user equipment suitable for worldwide use;
- user-friendly applications, services and equipment;
- worldwide roaming capability;
- enhanced peak data rates to support advanced services and applications (100 Mbit/s for high and 1 Gbit/s for low mobility were established as targets for research)¹.

These features enable IMT-Advanced to address evolving user needs.

The capabilities of IMT-Advanced systems are being continuously enhanced in line with user trends and technology developments.

2 Scope

This Report provides guidelines for both the procedure and the criteria (technical, spectrum and service) to be used in evaluating the proposed IMT-Advanced radio interface technologies (RITs) or Sets of RITs (SRITs) for a number of test environments and deployment scenarios for evaluation. These test environments are chosen to simulate closely the more stringent radio operating environments. The evaluation procedure is designed in such a way that the overall performance of the candidate RIT/SRITs may be fairly and equally assessed on a technical basis. It ensures that the overall IMT-Advanced objectives are met.

This Report provides, for proponents, developers of candidate RIT/SRITs and evaluation groups, the common methodology and evaluation configurations to evaluate the proposed candidate RIT/SRITs and system aspects impacting the radio performance.

¹ Data rates sourced from Recommendation ITU-R M.1645.

This Report allows a degree of freedom so as to encompass new technologies. The actual selection of the candidate RIT/SRITs for IMT-Advanced is outside the scope of this Report.

The candidate RIT/SRITs will be assessed based on those evaluation guidelines. If necessary, additional evaluation methodologies may be developed by each independent evaluation group to complement the evaluation guidelines. Any such additional methodology should be shared between evaluation groups and sent to the Radiocommunication Bureau as information in the consideration of the evaluation results by ITU-R and for posting under additional information relevant to the evaluation group section of the ITU-R IMT-Advanced web page (<http://www.itu.int/ITU-R/go/rsg5-imt-advanced>).

3 Structure of the Report

Section 4 provides a list of the documents that are related to this Report.

Section 5 describes the evaluation guidelines.

Section 6 lists the criteria chosen for evaluating the RITs.

Section 7 outlines the procedures and evaluation methodology for evaluating the criteria.

Section 8 defines the tests environments and selected deployment scenarios for evaluation; the evaluation configurations which shall be applied when evaluating IMT-Advanced candidate technology proposals are also given in this section.

Section 9 describes a channel model approach for the evaluation.

Section 10 provides a list of references.

Section 11 provides a list of acronyms and abbreviations.

Annexes 1 and 2 form a part of this Report.

4 Related ITU-R texts

Resolution ITU-R 57

Recommendation ITU-R M.1224

Recommendation ITU-R M.1822

Recommendation ITU-R M.1645

Recommendation ITU-R M.1768

Report ITU-R M.2038

Report ITU-R M.2072

Report ITU-R M.2074

Report ITU-R M.2078

Report ITU-R M.2079

Report ITU-R M.2133

Report ITU-R M.2134.

5 Evaluation guidelines

IMT-Advanced can be considered from multiple perspectives, including the users, manufacturers, application developers, network operators, and service and content providers as noted in § 4.2.2 in Recommendation ITU-R M.1645 – Framework and overall objectives of the future development of IMT-2000 and systems beyond IMT-2000. Therefore, it is recognized that the technologies for

IMT-Advanced can be applied in a variety of deployment scenarios and can support a range of environments, different service capabilities, and technology options. Consideration of every variation to encompass all situations is therefore not possible; nonetheless the work of the ITU-R has been to determine a representative view of IMT-Advanced consistent with the process defined in Resolution ITU-R 57 – Principles for the process of development of IMT-Advanced, and the requirements defined in Report ITU-R M.2134 – Requirements related to technical performance for IMT-Advanced radio interface(s).

The parameters presented in this Report are for the purpose of consistent definition, specification, and evaluation of the candidate RITs/SRITs for IMT-Advanced in ITU-R in conjunction with the development of Recommendations and Reports such as the framework and key characteristics and the detailed specifications of IMT-Advanced. These parameters have been chosen to be representative of a global view of IMT-Advanced but are not intended to be specific to any particular implementation of an IMT-Advanced technology. They should not be considered as the values that must be used in any deployment of any IMT-Advanced system nor should they be taken as the default values for any other or subsequent study in ITU or elsewhere.

Further consideration has been given in the choice of parameters to balancing the assessment of the technology with the complexity of the simulations while respecting the workload of an evaluator or technology proponent.

This procedure deals only with evaluating radio interface aspects. It is not intended for evaluating system aspects (including those for satellite system aspects).

The following principles are to be followed when evaluating radio interface technologies for IMT-Advanced:

- Evaluations of proposals can be through simulation, analytical and inspection procedures.
- The evaluation shall be performed based on the submitted technology proposals, and should follow the evaluation guidelines, use the evaluation methodology and adopt the evaluation configurations defined in this Report.
- Evaluations through simulations contain both system level simulations and link level simulations. Evaluation groups may use their own simulation tools for the evaluation.
- In case of analytical procedure the evaluation is to be based on calculations using the technical information provided by the proponent.
- In case of evaluation through inspection the evaluation is based on statements in the proposal.

The following options are foreseen for the groups doing the evaluations.

- Self-evaluation must be a complete evaluation (to provide a fully complete compliance template) of the technology proposal.
- An external evaluation group may perform complete or partial evaluation of one or several technology proposals to assess the compliance of the technologies with the minimum requirements of IMT-Advanced.
- Evaluations covering several technology proposals are encouraged.

6 Characteristics for evaluation

The technical characteristics chosen for evaluation are explained in detail in Report ITU-R M.2133 – Requirements, evaluation criteria and submission templates for the development of IMT-Advanced, § 2, including service aspect requirements which are based on Recommendation ITU-R M.1822, spectrum aspect requirements, and requirements related to technical performance,

which are based on Report ITU-R M.2134. These are summarised in Table 6-1, together with the high level assessment method:

- Simulation (including system and link-level simulations, according to the principles of simulation procedure given in § 7.1).
- Analytical (via a calculation).
- Inspection (by reviewing the functionality and parameterisation of the proposal).

TABLE 6-1

Characteristic for evaluation	Method	Evaluation methodology / configurations	Related section of Reports ITU-R M.2134 and ITU-R M.2133
Cell spectral efficiency	Simulation (system level)	§ 7.1.1, Tables 8-2, 8-4 and 8-5	Report ITU-R M.2134, § 4.1
Peak spectral efficiency	Analytical	§ 7.3.1, Table 8-3	Report ITU-R M.2134, § 4.2
Bandwidth	Inspection	§ 7.4.1	Report ITU-R M.2134, § 4.3
Cell edge user spectral efficiency	Simulation (system level)	§ 7.1.2, Tables, 8-2, 8-4 and 8-5	Report ITU-R M.2134, § 4.4
Control plane latency	Analytical	§ 7.3.2, Table 8-2	Report ITU-R M.2134, § 4.5.1
User plane latency	Analytical	§ 7.3.3; Table 8-2	Report ITU-R M.2134, § 4.5.2
Mobility	Simulation (system and link level)	§ 7.2, Tables 8-2 and 8-7	Report ITU-R M.2134, § 4.6
Intra- and inter-frequency handover interruption time	Analytical	§ 7.3.4, Table 8-2	Report ITU-R M.2134, § 4.7
Inter-system handover	Inspection	§ 7.4.3	Report ITU-R M.2134, § 4.7
VoIP capacity	Simulation (system level)	§ 7.1.3, Tables 8-2, 8-4 and 8-6	Report ITU-R M.2134, § 4.8
Deployment possible in at least one of the identified IMT bands	Inspection	§ 7.4.2	Report ITU-R M.2133, § 2.2
Channel bandwidth scalability	Inspection	§ 7.4.1	Report ITU-R M.2134, § 4.3
Support for a wide range of services	Inspection	§ 7.4.4	Report ITU-R M.2133, § 2.1

Section 7 defines the methodology for assessing each of these criteria.

7 Evaluation methodology

The submission and evaluation process is defined in Document IMT-ADV/2(Rev.1) –Submission and evaluation process and consensus building.

Evaluation should be performed in strict compliance with the technical parameters provided by the proponents and the evaluation configurations specified for the deployment scenarios in § 8.4 of this Report. Each requirement should be evaluated independently, except for the cell spectral efficiency and cell edge user spectral efficiency criteria that shall be assessed jointly using the same simulation, and that consequently the candidate RIT/SRITs also shall fulfil the corresponding minimum requirements jointly. Furthermore, the system simulation used in the mobility evaluation should be the same as the system simulation for cell spectral efficiency and cell edge user spectral efficiency.

The evaluation methodology should include the following elements:

- 1 Candidate RIT/SRITs should be evaluated using reproducible methods including computer simulation, analytical approaches and inspection of the proposal.
- 2 Technical evaluation of the candidate RIT/SRITs should be made against each evaluation criterion for the required test environments.
- 3 Candidate RIT/SRITs should be evaluated based on technical descriptions that are submitted using a technologies description template.

In order to have a good comparability of the evaluation results for each proposal, the following solutions and enablers are to be taken into account:

- Use of unified methodology, software, and data sets by the evaluation groups wherever possible, e.g. in the area of channel modelling, link-level data, and link-to-system-level interface.
- Evaluation of multiple proposals using one simulation tool by each evaluation group is encouraged.
- Question-oriented working method that adapts the level of detail in modelling of specific functionalities according to the particular requirements of the actual investigation.

Evaluation of cell spectral efficiency, peak spectral efficiency, cell edge user spectral efficiency and VoIP capacity of candidate RIT/SRITs should take into account the Layer 1 and Layer 2 overhead information provided by the proponents, which may vary when evaluating different performance metrics and deployment scenarios.

7.1 System simulation procedures

System simulation shall be based on the network layout defined in § 8.3 of this Report. The following principles shall be followed in system simulation:

- Users are dropped independently with uniform distribution over predefined area of the network layout throughout the system. Each mobile corresponds to an active user session that runs for the duration of the drop.
- Mobiles are randomly assigned LoS and NLoS channel conditions.
- Cell assignment to a user is based on the proponent's cell selection scheme, which must be described by the proponent.
- The minimum distance between a user and a base station is defined in Table 8-2 in § 8.4 of this Report.
- Fading signal and fading interference are computed from each mobile station into each cell and from each cell into each mobile station (in both directions on an aggregated basis).
- The IoT^2 (interference over thermal) parameter is an uplink design constraint that the proponent must take into account when designing the system such that the average IoT value experienced in the evaluation is equal to or less than 10 dB.
- In simulations based on the full-buffer traffic model, packets are not blocked when they arrive into the system (i.e. queue depths are assumed to be infinite).
- Users with a required traffic class shall be modelled according to the traffic models defined in Annex 2.

² The interference means the effective interference received at the base station.

- Packets are scheduled with an appropriate packet scheduler(s) proposed by the proponents for full buffer and VoIP traffic models separately. Channel quality feedback delay, feedback errors, PDU (protocol data unit) errors and real channel estimation effects inclusive of channel estimation error are modelled and packets are retransmitted as necessary.
- The overhead channels (i.e., the overhead due to feedback and control channels) should be realistically modelled.
- For a given drop the simulation is run and then the process is repeated with the users dropped at new random locations. A sufficient number of drops are simulated to ensure convergence in the user and system performance metrics. The proponent should provide information on the width of confidence intervals of user and system performance metrics of corresponding mean values, and evaluation groups are encouraged to provide this information.³
- Performance statistics are collected taking into account the wrap-around configuration in the network layout, noting that wrap-around is not considered in the indoor case.
- All cells in the system shall be simulated with dynamic channel properties using a wrap-around technique, noting that wrap-around is not considered in the indoor case.

In order to perform less complex system simulations, often the simulations are divided into separate ‘link’ and ‘system’ simulations with a specific link-to-system interface. Another possible way to reduce system simulation complexity is to employ simplified interference modelling. Such methods should be sound in principle, and it is not within the scope of this document to describe them.

Evaluation groups are allowed to use such approaches provided that the used methodologies are:

- well described and made available to the Radiocommunication Bureau and other evaluation groups;
- included in the evaluation report.

Realistic link and system models should include error modelling, e.g., for channel estimation and for the errors of control channels that are required to decode the traffic channel (including the feedback channel and channel quality information). The overheads of the feedback channel and the control channel should be modelled according to the assumptions used in the overhead channels’ radio resource allocation.

7.1.1 Cell spectral efficiency

The results from the system simulation are used to calculate the cell spectral efficiency as defined in Report ITU-R M.2134, § 4.1. The necessary information includes the number of correctly received bits during the simulation period and the effective bandwidth which is the operating bandwidth normalised appropriately considering the uplink/downlink ratio for TDD system.

Layer 1 and Layer 2 overhead should be accounted for in time and frequency for the purpose of calculation of system performance metrics such as cell spectral efficiency, cell edge user spectral efficiency, and VoIP. Examples of Layer 1 overhead include synchronization, guard and DC subcarriers, guard/switching time (in TDD systems), pilots and cyclic prefix. Examples of Layer 2 overhead include common control channels, HARQ ACK/NACK signalling, channel feedback, random access, packet headers and CRC. It must be noted that in computing the overheads, the fraction of the available physical resources used to model control overhead in Layer 1 and Layer 2

³ The confidence interval and the associated confidence level indicate the reliability of the estimated parameter value. The confidence level is the certainty (probability) that the true parameter value is within the confidence interval. The higher the confidence level the larger the confidence interval.

should be accounted for in a non-overlapping way. Power allocation/boosting should also be accounted for in modelling resource allocation for control channels.

7.1.2 Cell edge user spectral efficiency

The results from the system simulation are used to calculate the cell edge user spectral efficiency as defined in Report ITU-R M.2134, § 4.4. The necessary information is the number of correctly received bits per user during the active session time the user is in the simulation. The effective bandwidth is the operating bandwidth normalised appropriately considering the uplink/downlink ratio for TDD system. It should be noted that the cell edge user spectral efficiency shall be evaluated using identical simulation assumptions as the cell spectral efficiency for that test environment.

Examples of Layer 1 and Layer 2 overhead can be found in § 7.1.1.

7.1.3 VoIP capacity

The VoIP capacity should be evaluated and compared against the requirements in Report ITU-R M.2134, § 4.8.

VoIP capacity should be evaluated for the uplink and downlink directions assuming a 12.2 kbit/s codec with a 50% activity factor such that the percentage of users in outage is less than 2%, where a user is defined to have experienced a voice outage if less than 98% of the VoIP packets have been delivered successfully to the user within a permissible VoIP packet delay bound of 50 ms. The VoIP packet delay is the overall latency from the source coding at the transmitter to successful source decoding at the receiver.

The final VoIP capacity which is to be compared against the requirements in Report ITU-R M.2134 is the minimum of the calculated capacity for either link direction divided by the effective bandwidth in the respective link direction⁴.

The simulation is run with the duration for a given drop defined in Table 8-6 of this Report. The VoIP traffic model is defined in Annex 2.

7.2 Evaluation methodology for mobility requirements

The evaluator shall perform the following steps in order to evaluate the mobility requirement.

Step 1: Run system simulations, identical to those for cell spectral efficiencies, see § 7.1.1 except for speeds taken from Table 4 of Report ITU-R M.2134, using link level simulations and a link-to-system interface appropriate for these speed values, for the set of selected test environment(s) associated with the candidate RIT/SRIT proposal and collect overall statistics for uplink C/I values, and construct cumulative distribution function (CDF) over these values for each test environment.

Step 2: Use the CDF for the test environment(s) to save the respective 50%-percentile C/I value.

Step 3: Run new uplink link-level simulations for the selected test environment(s) for both NLoS and LoS channel conditions using the associated speeds in Table 4 of Report ITU-R M.2134, § 4.6 as input parameters, to obtain link data rate and residual packet error rate as a function of C/I . The link-level simulation shall use air interface configuration(s) supported by the proposal and take into account retransmission.

Step 4: Compare the link spectral efficiency values (link data rate normalized by channel bandwidth) obtained from Step 3 using the associated C/I value obtained from Step 2 for each

⁴ In other words, the effective bandwidth is the operating bandwidth normalised appropriately considering the uplink/downlink ratio for TDD systems.

channel model case, with the corresponding threshold values in the Table 4 of Report ITU-R M.2134, § 4.6.

Step 5: The proposal fulfils the mobility requirement if the spectral efficiency value is larger than or equal to the corresponding threshold value and if also the residual decoded packet error rate is less than 1%, for all selected test environments. For each test environment it is sufficient if one of the spectral efficiency values (of either NLoS or LoS channel conditions) fulfil the threshold.

7.3 Analytical approach

For the characteristics below a straight forward calculation based on the definition in Report ITU-R M.2134 and information in the proposal will be enough to evaluate them. The evaluation shall describe how this calculation has been performed. Evaluation groups should follow the calculation provided by proponents if it is justified properly.

7.3.1 Peak spectral efficiency calculation

The peak spectral efficiency is calculated as specified in Report ITU-R M.2134 § 4.2. The antenna configuration to be used for peak spectral efficiency is defined in Table 8-3 of this Report. The necessary information includes effective bandwidth which is the operating bandwidth normalised appropriately considering the uplink/downlink ratio for TDD systems. Examples of Layer 1 overhead can be found in § 7.1.1.

7.3.2 Control plane latency calculation

The control plane latency is calculated as specified in Report ITU-R M.2134, § 4.5.1.

The proponent should provide the elements in the calculation of the control plane latency and the retransmission probability.

Table 7-1 provides, for the purpose of example, typical elements in the calculation of the control plane latency. The inclusion of H-ARQ/ARQ retransmissions in each step of the connection set up is to ensure the required reliability of connection which typically has a probability of error in the order of 10^{-2} for certain Layer 2 control signals and 10^{-6} for some RRC control signals.

TABLE 7-1

Example C-plane latency template

Step	Description	Duration
0	UT wakeup time	Implementation dependent
1	DL scanning and synchronization + Broadcast channel acquisition	
2	Random access procedure	
3	UL synchronization	
4	Capability negotiation + H-ARQ retransmission probability	
5	Authorization and authentication/key exchange +H-ARQ retransmission probability	
6	Registration with the BS + H-ARQ retransmission probability	
7	RRC connection establishment + H-ARQ retransmission probability	
	Total C-plane connection establishment delay	
	Total IDLE_STATE → ACTIVE_ACTIVE delay	

7.3.3 User plane latency calculation

The user plane latency is calculated as specified in Report ITU-R M.2134, § 4.5.2. The proponent should provide the elements in the calculation of the user plane latency and the retransmission probability.

Table 7-2 provides, for the purpose of example, typical elements in the calculation of the user plane latency:

TABLE 7-2
Example user-plane latency analysis template

Step	Description	Value
0	UT wakeup time	Implementation dependent
1	UT processing delay	
2	Frame alignment	
3	TTI for UL data packet (piggy-back scheduling information)	
4	HARQ retransmission (probability)	
5	BS processing delay	
6	Transfer delay between the BS and the BS-Core Network interface	
7	Processing delay of the BS-Core Network interface	
	Total one way delay	

7.3.4 Intra- and inter-frequency handover interruption time derivation

The intra- and inter-frequency handover interruption time is calculated as specified in Report ITU-R M.2134, § 4.7. The handover procedure shall be described based on the proposed technology including the functions and the timing involved.

7.4 Inspection

7.4.1 Bandwidth and channel bandwidth scalability

The support of maximum bandwidth required in Report ITU-R M.2134, § 4.3 is verified by inspection of the proposal.

The scalability requirement is verified by demonstrating that the candidate RIT or SRIT can support at least three bandwidth values. These values shall include the minimum and maximum supported bandwidth values of the candidate RIT or SRIT.

7.4.2 Deployment in IMT bands

The set of IMT bands supported is demonstrated by inspection of the proposal.

7.4.3 Inter-system handover

The support of inter-system handover as required in Report ITU-R M.2134, § 4.7 is verified by inspection of the proposal.

7.4.4 Support of a wide range of services

A mobile transmission system's ability to support a wide range of services lies across all elements of the network (i.e. core, distribution and access), and across all layers of the OSI model. The evaluation of a candidate IMT-Advanced RIT focuses on the radio access aspects of the lower OSI layers. There are quantifiable elements of the minimum technical requirements identified within Report ITU-R M.2134 that indicate whether or not a candidate RIT is capable of enabling these services as defined in Recommendation ITU-R M.1822. If the candidate RIT meets the latency, peak spectral efficiency and bandwidth requirements in Report ITU-R M.2134, then it can be regarded as enabling the following service aspects requirements.

The support of a wide range of services is further analysed by inspection of the candidate RIT's ability to support all of the service classes of Table 7-3. This is considered in at least one test environment (similar to evaluation of the peak spectral efficiency) under normal operating conditions using configuration supported by the candidate RIT/SRITs.

TABLE 7-3

Service classes for evaluation

User experience class	Service class	Inspection
Conversational	Basic conversational service	Yes/No
	Rich conversational service	Yes/No
	Conversational low delay	Yes/No
Interactive	Interactive high delay	Yes/No
	Interactive low delay	Yes/No
Streaming	Streaming live	Yes/No
	Streaming non-live	Yes/No
Background	Background	Yes/No

8 Test environments and evaluation configurations

This section describes the test environments, selected deployment scenarios and evaluation configurations (including simulation parameters) necessary to evaluate the performance figures of candidate RIT/SRITs (details of test environments and channel models can be found in Annex 1).

The predefined test environments are used in order to specify the environments of the requirements for the technology proposals. IMT-Advanced is to cover a wide range of performance in a wide range of environments. Although it should be noted that thorough testing and evaluation is prohibitive. The test environments have therefore been chosen such that typical and different deployments are modelled and critical questions in system design and performance can be investigated. Focus is thus on scenarios testing limits of performance related to capacity and user mobility.

8.1 Test environments

Evaluation of candidate RIT/SRITs will be performed in selected scenarios of the following test environments:

- **Indoor:** an indoor environment targeting isolated cells at offices and/or in hotspot based on stationary and pedestrian users.
- **Microcellular:** an urban micro-cellular environment with higher user density focusing on pedestrian and slow vehicular users.
- **Base coverage urban:** an urban macro-cellular environment targeting continuous coverage for pedestrian up to fast vehicular users.
- **High speed:** macro cells environment with high speed vehicular and trains.

8.1.1 Indoor test environment

The indoor test environment focuses on smallest cells and high user throughput or user density in buildings. The key characteristics of this test environment are high user throughput or user density in indoor coverage.

8.1.2 Microcellular test environment

The microcellular test environment focuses on small cells and high user densities and traffic loads in city centres and dense urban areas. The key characteristics of this test environment are high traffic loads, outdoor and outdoor-to-indoor coverage. This scenario will therefore be interference-limited, using micro cells. A continuous cellular layout and the associated interference shall be assumed. Radio access points shall be below rooftop level.

A similar scenario is used to the base coverage urban test environment but with reduced site-to-site distance and the antennas below rooftops.

8.1.3 Base coverage urban test environment

The base coverage urban test environment focuses on large cells and continuous coverage. The key characteristics of this test environment are continuous and ubiquitous coverage in urban areas. This scenario will therefore be interference-limited, using macro cells (i.e. radio access points above rooftop level).

In urban macro-cell scenario mobile station is located outdoors at street level and fixed base station antenna clearly above surrounding building heights. As for propagation conditions, non- or obstructed line-of-sight is a common case, since street level is often reached by a single diffraction over the rooftop.

8.1.4 High-speed test environment

The high-speed test environment focuses on larger cells and continuous coverage. The key characteristics of this test environment are continuous wide area coverage supporting high speed vehicles. This scenario will therefore be noise-limited and/or interference-limited, using macro cells.

8.2 Deployment scenarios for the evaluation process

The deployment scenarios that shall be used for each test environment are shown in Table 8-1:

TABLE 8-1

Selected deployment scenarios for evaluation

Test environment	Indoor	Microcellular	Base coverage urban	High speed
Deployment scenario	Indoor hotspot scenario	Urban micro-cell scenario	Urban macro-cell scenario	Rural macro-cell scenario

Suburban macro-cell scenario is an optional scenario for the base coverage urban test environment.

8.3 Network layout

In the rural/high-speed, base coverage urban and microcell cases, no specific topographical details are taken into account. Base stations are placed in a regular grid, following hexagonal layout. A basic hexagon layout for the example of three cells per site is shown in Fig. 1, where also basic geometry (antenna boresight, cell range, and inter-site distance ISD) is defined. The simulation will be a wrap-around configuration of 19 sites, each of 3 cells. Users are distributed uniformly over the whole area.

The amount of channel bandwidth used in a link direction that is used in the simulation is defined as the product of the spectrum bandwidth identified in the tables (Tables 8-5, 8-6, 8-7) as “simulation bandwidth” and the frequency reuse factor, when conventional frequency reuse scheme (e.g. 3-cell

and 7-cell frequency reuse) is considered. The cell spectral efficiency, cell edge user spectral efficiency, and VoIP capacity are calculated taking into account the amount of channel bandwidth used for each link direction.

Consider as an example the urban macro cell scenario column for full buffer services in Table 8-5. According to this table the simulation bandwidths are 10 + 10 MHz for FDD and 20 MHz for TDD based systems.

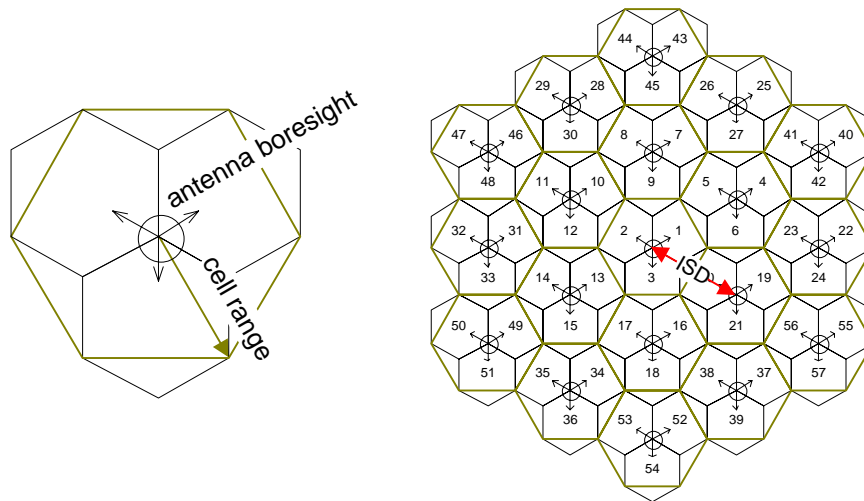
Assuming that an FDD based proposal has frequency reuse factor 3 the resulting amount of spectrum is $3 \times 10 = 30$ MHz for each link, or 60 MHz summed over both directions.

Alternatively, assuming a TDD based proposal with frequency reuse factor of 3 the resulting amount of spectrum is $3 \times 20 = 60$ MHz (also used for both directions). The fraction of time each link direction is taken into account. However, for TDD also the fraction of time each link direction is active should be taken into account to get the effective bandwidth (as an example, the proponent could specify these figures as 60% for UL transmissions and 40% for DL transmissions).

When calculating spectral efficiencies and VoIP capacities for FDD the total spectrum for each individual link should be used in the calculation (30 MHz for each direction in the example), while for TDD the amount of spectrum used for any link direction should be used (60 MHz in the example).

FIGURE 1

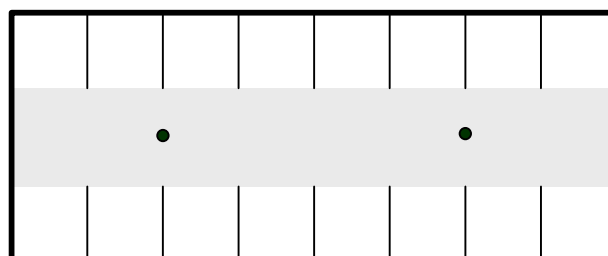
Sketch of base coverage urban cell layout without relay nodes



The indoor hotspot scenario consists of one floor of a building. The height of the floor is 6 m. The floor contains 16 rooms of 15 m × 15 m and a long hall of 120 m × 20 m. Two sites are placed in the middle of the hall at 30 m and 90 m with respect to the left side of the building (see Fig. 2).

FIGURE 2

Sketch of indoor hotspot environment (one floor)



8.4 Evaluation configurations

This section contains baseline configuration parameters that shall be applied in analytical and simulation assessments of candidate RIT/SRITs.

The parameters (and also the propagation and channel models in Annex 1) are solely for the purpose of consistent evaluation of the candidate RIT/SRITs and relate only to specific test environments used in these simulations. They should not be considered as the values that must be used in any deployment of any IMT-Advanced system nor should they taken as the default values for any other or subsequent study in ITU or elsewhere. They do not necessarily themselves constitute any requirements on the implementation of the system.

Configuration parameters in Table 8-2 shall be applied when evaluation groups assess the characteristics of cell spectral efficiency, cell edge user spectral efficiency, control plane latency, user plane latency, mobility, handover interruption time and VoIP capacity in evaluation of candidate RIT/SRITs.

TABLE 8-2

Baseline evaluation configuration parameters

Deployment scenario for the evaluation process	Indoor hotspot	Urban micro-cell	Urban macro-cell	Rural macro-cell	Suburban macro-cell
Base station (BS) antenna height	6 m, mounted on ceiling	10 m, below rooftop	25 m, above rooftop	35 m, above rooftop	35 m, above rooftop
Number of BS antenna elements ⁽¹⁾	Up to 8 rx Up to 8 tx	Up to 8 rx Up to 8 tx	Up to 8 rx Up to 8 tx	Up to 8 rx Up to 8 tx	Up to 8 rx Up to 8 tx
Total BS transmit power	24 dBm for 40 MHz, 21 dBm for 20 MHz	41 dBm for 10 MHz, 44 dBm for 20 MHz	46 dBm for 10 MHz, 49 dBm for 20 MHz	46 dBm for 10 MHz, 49 dBm for 20 MHz	46 dBm for 10 MHz, 49 dBm for 20 MHz
User terminal (UT) power class	21 dBm	24 dBm	24 dBm	24 dBm	24 dBm
UT antenna system ⁽¹⁾	Up to 2 tx Up to 2 rx	Up to 2 tx Up to 2 rx	Up to 2 tx Up to 2 rx	Up to 2 tx Up to 2 rx	Up to 2 tx Up to 2 rx
Minimum distance between UT and serving cell ⁽²⁾	≥ 3 m	≥ 10 m	≥ 25 m	≥ 35 m	≥ 35 m
Carrier frequency (CF) for evaluation (representative of IMT bands)	3.4 GHz	2.5 GHz	2 GHz	800 MHz	Same as urban macro-cell
Outdoor to indoor building penetration loss	N.A.	See Annex 1, Table A1-2	N.A.	N.A.	20 dB
Outdoor to in-car penetration loss	N.A.	N.A.	9 dB (LN, $\sigma = 5$ dB)	9 dB (LN, $\sigma = 5$ dB)	9 dB (LN, $\sigma = 5$ dB)

(1) The number of antennas specified by proponent in the technology description template (§ 4.2.3 of Report ITU-R M.2133) should be used in the evaluations. The numbers shall be within the indicated ranges in this table.

(2) In the horizontal plane.

8.4.1 Evaluation configurations parameters for analytical assessment

Configuration parameters in Table 8-3 shall be applied when evaluation groups assess the characteristics of peak spectral efficiency in evaluation of candidate RIT/SRITs.

TABLE 8-3

Evaluation configuration parameters for analytical assessment of peak spectral efficiency

Deployment scenario for the evaluation process	Indoor hotspot	Urban micro-cell	Urban macro-cell	Rural macro-cell	Suburban macro-cell
Number of BS antenna elements	Up to 4 rx	Up to 4 rx	Up to 4 rx	Up to 4 rx	Up to 4 rx
	Up to 4 tx	Up to 4 tx	Up to 4 tx	Up to 4 tx	Up to 4 tx
UT antenna system	Up to 2 tx	Up to 2 tx	Up to 2 tx	Up to 2 tx	Up to 2 tx
	Up to 4 rx	Up to 4 rx	Up to 4 rx	Up to 4 rx	Up to 4 rx

8.4.2 Evaluation configurations parameters for simulation assessment

There are two types of simulations: system simulation and link level simulation.

8.4.2.1 Additional parameters for system simulation

Parameters in Table 8-4 shall also be applied in system simulation when assessing the characteristics of cell spectral efficiency, cell edge user spectral efficiency and VoIP capacity.

TABLE 8-4

Additional parameters for system simulation

Deployment scenario for the evaluation process	Indoor hotspot	Urban micro-cell	Urban macro-cell	Rural macro-cell	Suburban macro-cell
Layout ⁽¹⁾	Indoor floor	Hexagonal grid	Hexagonal grid	Hexagonal grid	Hexagonal grid
Inter-site distance	60 m	200 m	500 m	1 732 m	1 299 m
Channel model	Indoor hotspot model (InH)	Urban micro model (UMi)	Urban macro model (UMa)	Rural macro model (RMa)	Suburban macro model (SMa)
User distribution	Randomly and uniformly distributed over area	Randomly and uniformly distributed over area. 50% users outdoor (pedestrian users) and 50% of users indoors	Randomly and uniformly distributed over area. 100% of users outdoors in vehicles	Randomly and uniformly distributed over area. 100% of users outdoors in high speed vehicles	Randomly and uniformly distributed over area. 50% users vehicles and 50% of users indoors
User mobility model	Fixed and identical speed $ v $ of all UTs, randomly and uniformly distributed direction	Fixed and identical speed $ v $ of all UTs, randomly and uniformly distributed direction	Fixed and identical speed $ v $ of all UTs, randomly and uniformly distributed direction	Fixed and identical speed $ v $ of all UTs, randomly and uniformly distributed direction	Fixed and identical speed $ v $ of all UTs, randomly and uniformly distributed direction
UT speeds of interest	3 km/h	3 km/h	30 km/h	120 km/h	Indoor UTs: 3 km/h, outdoor UTs: 90 km/h
Inter-site interference modeling ⁽²⁾	Explicitly modelled	Explicitly modelled	Explicitly modelled	Explicitly modelled	Explicitly modelled

TABLE 8-4 (*end*)

Deployment scenario for the evaluation process	Indoor hotspot	Urban micro-cell	Urban macro-cell	Rural macro-cell	Suburban macro-cell
BS noise figure	5 dB	5 dB	5 dB	5 dB	5 dB
UT noise figure	7 dB	7 dB	7 dB	7 dB	7 dB
BS antenna gain (boresight)	0 dBi	17 dBi	17 dBi	17 dBi	17 dBi
UT antenna gain	0 dBi	0 dBi	0 dBi	0 dBi	0 dBi
Thermal noise level	-174 dBm/Hz	-174 dBm/Hz	-174 dBm/Hz	-174 dBm/Hz	-174 dBm/Hz

(1) See § 8.3 for further detail.

(2) See § 7.1.

When assessing the cell spectral efficiency and cell edge user spectral efficiency characteristics, parameters in Table 8-5 shall also be applied.

TABLE 8-5

**Additional parameters for assessment of cell spectral efficiency
and cell edge user spectral efficiency**

Deployment scenario for the evaluation process	Indoor hotspot	Urban micro-cell	Urban macro-cell	Rural macro-cell	Suburban macro-cell
Evaluated service profiles	Full buffer best effort	Full buffer best effort	Full buffer best effort	Full buffer best effort	Full buffer best effort
Simulation bandwidth	20 + 20 MHz (FDD), or 40 MHz (TDD)	10 + 10 MHz (FDD), or 20 MHz (TDD)	10 + 10 MHz (FDD), or 20 MHz (TDD)	10 + 10 MHz (FDD), or 20 MHz (TDD)	10 + 10 MHz (FDD), or 20 MHz (TDD)
Number of users per cell	10	10	10	10	10

The simulation needs to be done over a time period long enough to assure convergence of the simulation results.

When assessing the VoIP capacity characteristic, parameters in Table 8-6 shall also be applied.

TABLE 8-6

Additional parameters for assessment of VoIP capacity

Deployment scenario for the evaluation process	Indoor hotspot	Urban micro-cell	Urban macro-cell	Rural macro-cell	Suburban macro-cell
Evaluated service profiles	VoIP	VoIP	VoIP	VoIP	VoIP
Simulation bandwidth ⁽¹⁾	5 + 5 MHz (FDD), 10 MHz (TDD)	5 + 5 MHz (FDD), 10 MHz (TDD)	5 + 5 MHz (FDD), 10 MHz (TDD)	5 + 5 MHz (FDD), 10 MHz (TDD)	5 + 5 MHz (FDD), 10 MHz (TDD)
Simulation time span for a single drop	20 s	20 s	20 s	20 s	20 s

- (1) While it is recognized that the bandwidth associated with VoIP implementations could be significantly larger than the bandwidth specified herein; this bandwidth was chosen to allow simulations to be practically conducted. Using larger bandwidths and the corresponding larger number of users to be simulated increases the simulation complexity and time required to perform the simulations.

8.4.2.2 Additional parameters for link level simulation

Parameters in Table 8-7 shall also be applied in link level simulation when assessing the characteristic of mobility.

TABLE 8-7

Additional parameters for link level simulation (for mobility requirement)

Deployment scenario for the evaluation process	Indoor hotspot	Urban micro-cell	Urban macro-cell	Rural macro-cell	Suburban macro-cell
Evaluated service profiles	Full buffer best effort	Full buffer best effort	Full buffer best effort	Full buffer best effort	Full buffer best effort
Channel model	Indoor hotspot model (InH)	Urban micro-cell model (UMi)	Urban macro-cell model (UMa)	Rural macro-cell model (RMa)	Suburban macro-cell model (SMa)
Simulation bandwidth	10 MHz	10 MHz	10 MHz	10 MHz	10 MHz
Number of users in simulation	1	1	1	1	1

8.5 Antenna characteristics

This sub-section specifies the antenna characteristics, e.g. antenna pattern, gain, side-lobe level, orientation, etc., for antennas at the base station (BS) and the user terminal (UT), which shall be applied for the evaluation in the deployment scenarios with the hexagonal grid layout (i.e., urban macro-cell, urban micro-cell, rural macro-cell, and suburban macro-cell). The characteristics do not form any kind of requirements and should be used only for the evaluation.

8.5.1 BS antenna

8.5.1.1 BS antenna pattern

The horizontal antenna pattern used for each BS sector⁵ is specified as:

$$A(\theta) = -\min \left[12 \left(\frac{\theta}{\theta_{3\text{dB}}} \right)^2, A_m \right] \quad (1)$$

Where $A(\theta)$ is the relative antenna gain (dB) in the direction θ , $-180^\circ \leq \theta \leq 180^\circ$, and $\min [.]$ denotes the minimum function, $\theta_{3\text{dB}}$ is the 3 dB beamwidth (corresponding to $\theta_{3\text{dB}} = 70^\circ$), and $A_m = 20$ dB is the maximum attenuation. Figure 3 shows the BS antenna pattern for 3 sector cells to be used in system level simulations.

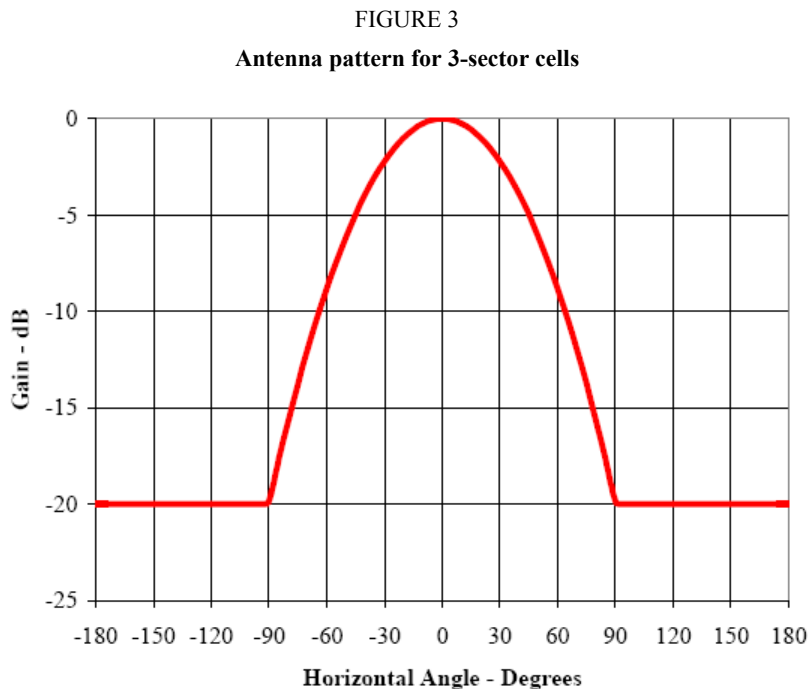
A similar antenna pattern will be used for elevation in simulations that need it. In this case the antenna pattern will be given by:

$$A_e(\phi) = -\min \left[12 \left(\frac{\phi - \phi_{\text{tilt}}}{\phi_{3\text{dB}}} \right)^2, A_m \right] \quad (2)$$

where $A_e(\phi)$ is the relative antenna gain (dB) in the elevation direction, ϕ , $-90^\circ \leq \phi \leq 90^\circ$, $\phi_{3\text{dB}}$. ϕ_{tilt} is the elevation 3 dB value, and it may be assumed to be 15° , unless stated otherwise. ϕ_{tilt} is the tilt angle, which should be provided by proponents per deployment scenario.

The combined antenna pattern at angles off the cardinal axes is computed as:

$$-\min \left[-\left(A(\theta) + A_e(\phi) \right), A_m \right]$$



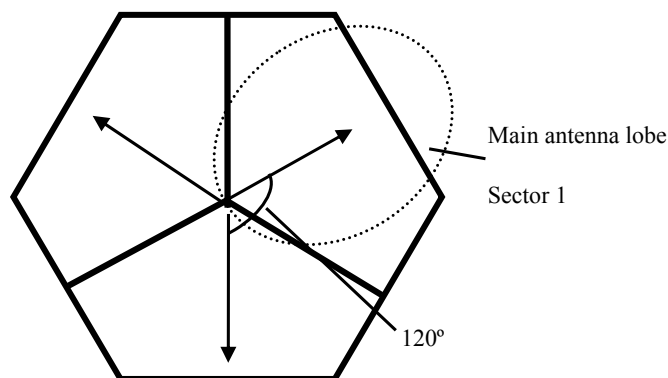
⁵ A sector is equivalent to a cell.

8.5.1.2 BS antenna orientation

The antenna bearing is defined as the angle between the main antenna lobe centre and a line directed due east given in degrees. The bearing angle increases in a clockwise direction. Figure 4 shows the hexagonal cell and its three sectors with the antenna bearing orientation proposed for the simulations. The centre directions of the main antenna lobe in each sector point to the corresponding side of the hexagon.

For indoor test environment, omni antenna should be used for the BS.

FIGURE 4
Antenna bearing orientation diagram



8.5.2 UT antenna

The UT antenna is assumed to be omni directional.

9 Channel model approach

Channel models are needed in the evaluations of the IMT-Advanced candidate radio interface technologies (RITs) to allow realistic modelling of the propagation conditions for the radio transmissions in different environments. The channel model needs to cover all required test environments and scenarios of the IMT-Advanced evaluations.

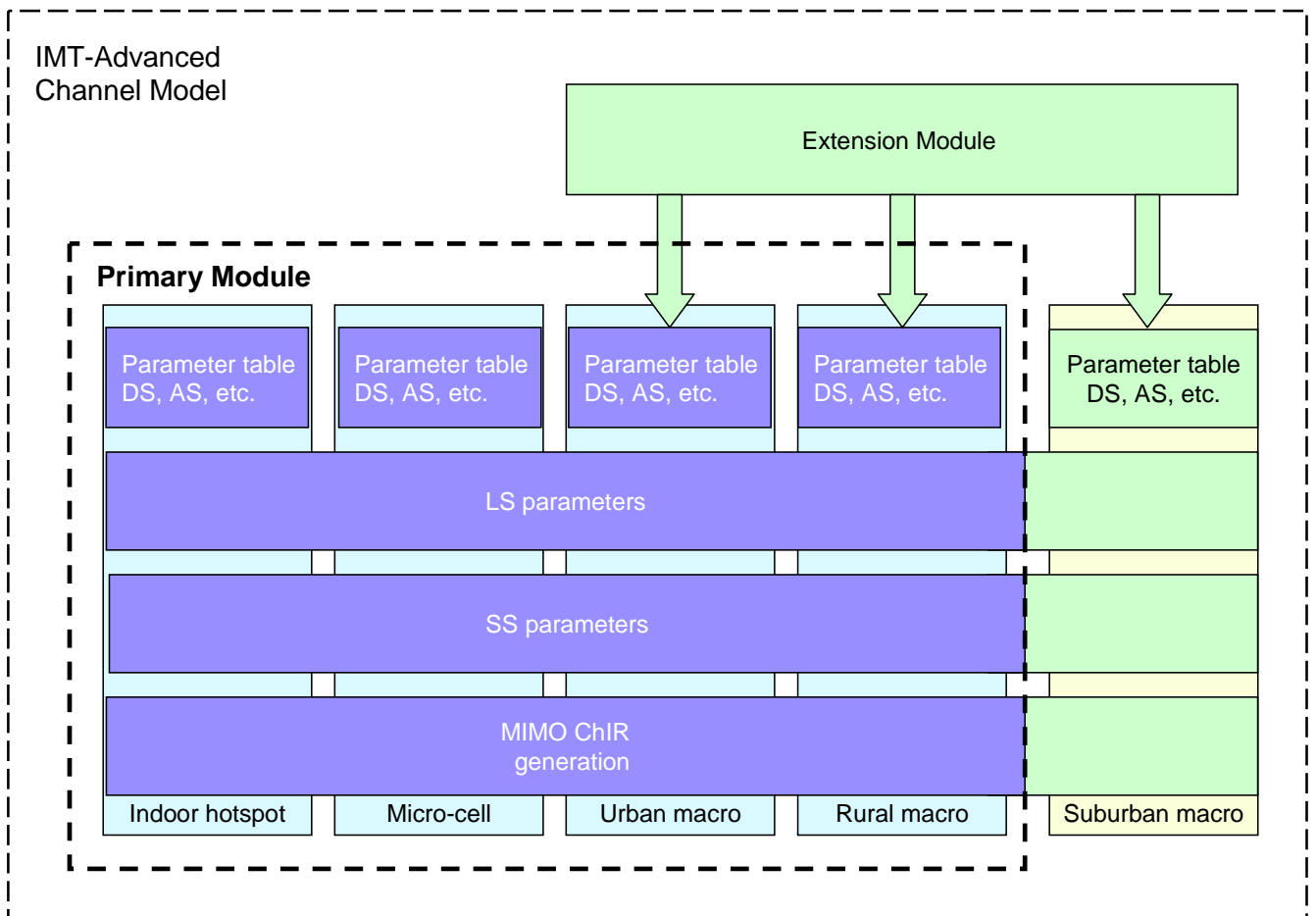
Realistic system performance cannot be evaluated by single link simulations. Even the performance of a single link depends on other links due to the influence of advanced radio resource management (RRM) algorithms, interference generated by other links and so on. Multi-link models for system level evaluations have been developed in the family of geometry-based stochastic channel models.

The IMT-Advanced channel model for the evaluation of IMT-Advanced candidate RITs consists of a Primary Module and an Extension Module as shown in Fig. 5. The framework of the primary module is based on the WINNER II channel model*, which applies the same approach as 3GPP/3GPP2 SCM model**. Different evaluation scenarios are shown in parallel in Fig. 5.

* IST-WINNER II Deliverable 1.1.2 v.1.2. WINNER II Channel Models, IST-WINNER2. Tech. Rep., 2007 (<http://www.ist-winner.org/deliverables.html>).

** 3GPP TR25.996 V6.1.0 (2003-09) Spatial channel model for multiple input multiple output (MIMO) simulations. Release 6.

FIGURE 5
The IMT-Advanced channel model



The scenarios chosen for the evaluations of the IMT-Advanced candidate RITs are: indoor hotspot, urban micro-cell, urban macro-cell and rural macro-cell. The primary module covers the parameter tables and channel model definition for the evaluations. The IMT-Advanced channel model contains parameters from Table A1-7 for evaluating the IMT-Advanced candidate RITs in the four scenarios of the primary module.

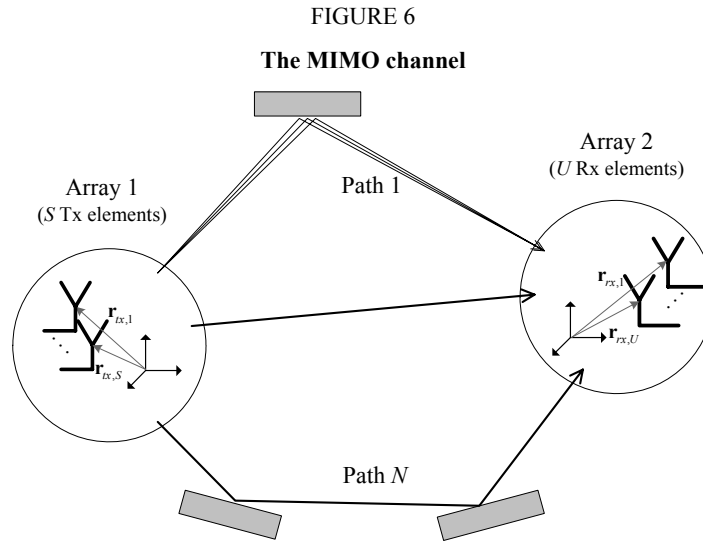
Mandatory channel model parameters for evaluation of RITs for the scenarios indoor hotspot, urban micro-cell, urban macro-cell, and rural macro-cell are contained in the primary module as shown in Fig. 5 and in Table A1-7 and are not generated from the extension module. In addition, the channel model could also be applied for other cases, i.e., if some of the parameters described in § 8.4 for macro-cell scenarios, e.g., BS antenna height, street width, city structure, etc. could be varied to cover other cases not described in this Report. The extension module can extend the capabilities of the IMT-Advanced channel model to cover those cases beyond the evaluations of the IMT-Advanced candidate RITs by allowing the usage of modified parameters to generate large scale parameters in the scenarios or usage of other scenarios.

The ITU-R IMT-Advanced channel model is a geometry-based stochastic model. It can also be called double directional channel model. It does not explicitly specify the locations of the scatterers, but rather the directions of the rays, like the well-known spatial channel model (SCM)*. Geometry-based modelling of the radio channel enables separation of propagation parameters and antennas.

* 3GPP TR25.996 V6.1.0 (2003-09) Spatial channel model for multiple input multiple output (MIMO) simulations. Release 6.

The channel parameters for individual snapshots are determined stochastically based on statistical distributions extracted from channel measurements. Antenna geometries and radiation patterns can be defined properly by the user of the model. Channel realizations are generated through the application of the geometrical principle by summing contributions of rays (plane waves) with specific small-scale parameters like delay, power, angle-of-arrival (AoA) and angle-of-departure (AoD). Superposition results to correlation between antenna elements and temporal fading with geometry dependent Doppler spectrum.

A number of rays constitute a cluster. In the terminology of this document we equate the cluster with a propagation path diffused in space, either or both in delay and angle domains. Elements of the MIMO channel, e.g., antenna arrays at both link ends and propagation paths, are illustrated in Fig. 6. The generic MIMO channel model is applicable for all scenarios, e.g. indoor, urban and rural.



The time variant impulse response matrix of the $U \times S$ MIMO channel is given by:

$$\mathbf{H}(t; \tau) = \sum_{n=1}^N \mathbf{H}_n(t; \tau) \quad (3)$$

where:

- t : time
- τ : delay
- N : number of paths
- n : path index.

It is composed of the antenna array response matrices \mathbf{F}_{tx} and \mathbf{F}_{rx} for the transmitter (Tx) and the receiver (Rx) respectively, and the dual-polarized propagation channel response matrix, \mathbf{h}_n , for cluster, n , as follows:

$$\mathbf{H}_n(t; \tau) = \iint \mathbf{F}_{rx}(\phi) \mathbf{h}_n(t; \tau, \phi, \varphi) \mathbf{F}_{tx}^T(\phi) d\phi d\varphi . \quad (4)$$

The channel from Tx antenna element, s , to Rx element, u , for cluster, n , is expressed as:

$$\begin{aligned}
 H_{u,s,n}(t; \tau) = & \sum_{m=1}^M \begin{bmatrix} F_{rx,u,V}(\phi_{n,m}) \\ F_{rx,u,H}(\phi_{n,m}) \end{bmatrix}^T \begin{bmatrix} \alpha_{n,m,VV} & \alpha_{n,m,VH} \\ \alpha_{n,m,HV} & \alpha_{n,m,HH} \end{bmatrix} \begin{bmatrix} F_{tx,s,V}(\phi_{n,m}) \\ F_{tx,s,H}(\phi_{n,m}) \end{bmatrix} \\
 & \times \exp(j2\pi\lambda_0^{-1}(\bar{\phi}_{n,m} \cdot \bar{r}_{rx,u})) \exp(j2\pi\lambda_0^{-1}(\bar{\phi}_{n,m} \cdot \bar{r}_{tx,s})) \\
 & \times \exp(j2\pi\nu_{n,m}t) \delta(\tau - \tau_{n,m})
 \end{aligned} \quad (5)$$

where:

- $F_{rx,u,V}$ and $F_{rx,u,H}$: antenna element u field patterns for vertical and horizontal polarizations respectively
- $\alpha_{n,m,VV}$ and $\alpha_{n,m,VH}$: complex gains of vertical-to-vertical and horizontal-to-vertical polarizations of ray n,m respectively
- λ_0 : wave length of the carrier frequency
- $\bar{\phi}_{n,m}$: AoD unit vector
- $\bar{\varphi}_{n,m}$: AoA unit vector
- $\bar{r}_{tx,s}$ and $\bar{r}_{rx,u}$: location vectors of element s and u respectively
- $\nu_{n,m}$: Doppler frequency component of ray n,m .

If the radio channel is modelled as dynamic, all the above mentioned small-scale parameters are time variant, i.e., they are functions of t [Steinbauer *et al.*, 2001].

The primary module covers the mathematical framework, which is called *generic model*, a set of parameters as well as path loss models. A reduced variability model with fixed parameters is also defined which is called *clustered delay line (CDL) model*. The CDL model cannot be used for evaluations of candidate RITs at the link level or system level, but it can be used for calibration purposes only.

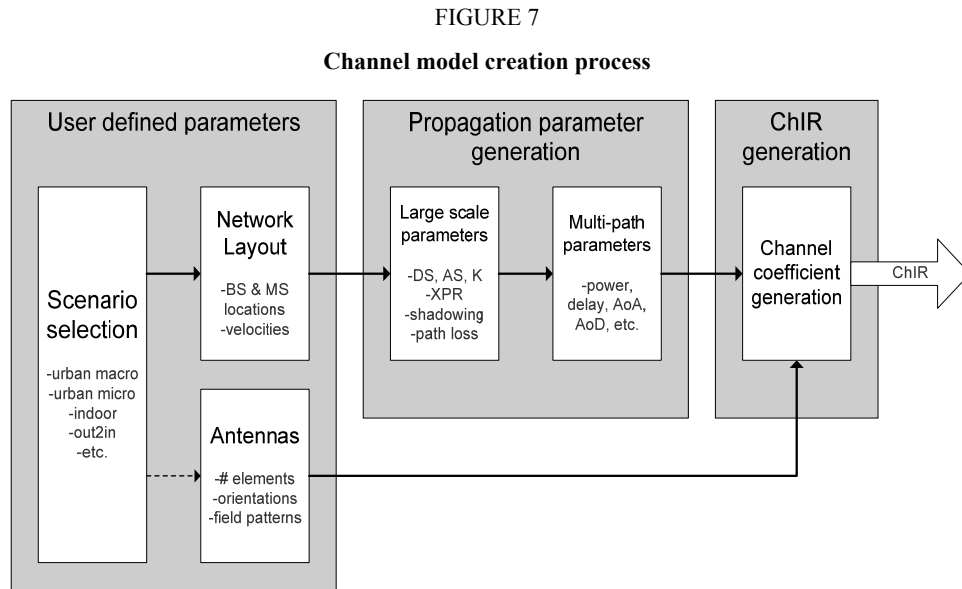
9.1 Generic channel model (mandatory)

The generic channel model is a double-directional geometry-based stochastic model. It is a system level⁶ model in the sense that is employed, e.g., in the SCM model*. It can describe an unlimited number of propagation environment realizations for single or multiple radio links for all the defined scenarios and for arbitrary antenna configurations, with one mathematical framework by different parameter sets. The generic channel model is a stochastic model with two (or three) levels of randomness. First, large-scale (LS) parameters like shadow fading, delay, and angular spreads are drawn randomly from tabulated distribution functions. Next, small-scale (SS) parameters like delays, powers, and directions of arrival and departure are drawn randomly according to tabulated distribution functions and random LS parameters. At this stage the geometric setup is fixed and the only free variables are the random initial phases of the scatterers. By picking (randomly) different initial phases, an infinite number of different realizations of the model can be generated. When the initial phases are also fixed, there is no further randomness left.

⁶ The term system-level means here that the model is able to cover multiple links, cells and terminals.

* IST-WINNER II Deliverable 1.1.2 v.1.2. WINNER II Channel Models, IST-WINNER2. Tech. Rep., 2008 (<http://www.ist-winner.org/deliverables.html>).

Figure 7 shows the overview of the channel model creation. The first stage consists of two steps. First, the propagation scenario is selected. Then, the network layout and the antenna configuration are determined. In the second stage, large-scale and small-scale parameters are defined. In the third stage, channel impulse responses (ChIRs) are calculated.



9.1.1 Drop concept

The generic model is based on the drop concept. When using the generic model, the simulation of the system behaviour is carried out as a sequence of “drops”, where a “drop” is defined as one simulation run over a certain time period. A drop (or snapshot or channel segment) is a simulation entity where the random properties of the channel remain constant except for the fast fading caused by the changing phases of the rays. The constant properties during a single drop are, e.g., the powers, delays, and directions of the rays. In a simulation the number and the length of drops have to be selected properly by the evaluation requirements and the deployed scenario. The generic model allows the user to simulate over several drops to get statistically representative results. Consecutive drops are independent.

9.2 CDL model (for calibration)

The generic model is aimed to be applicable for many different simulations and to cover a large number of scenarios with several combinations of large-scale and small-scale parameters. The generic model is the most accurate model and is used in all evaluations of candidate RITs. However, for calibration purposes, the CDL model can be used.

The CDL model is a spatial extension of tapped delay line (TDL) model. The TDL model usually contains power, delay, and Doppler spectrum information for the taps. CDL models define power, delay, and angular information. Doppler is not explicitly defined, because it is determined by power and angular information combined with array characteristics and mobile movement.

The CDL approach fixes all the parameters except for the phases of the rays, although other alternatives can be considered:

- the main direction of the rays can be made variable,
- a set of reference antenna geometries and antenna patterns can be proposed,
- relation to correlation-matrix based models can be introduced.

10 List of acronyms and abbreviations

ACK	Acknowledgment
AoA	Angle of arrival
AoD	Angle of departure
ARQ	Automatic repeat request
AS	Angle spread
ASA	Angle spread of arrival (AoA spread)
ASD	Angle spread of departure (AoD spread)
BS	Base station
CDD	Cyclic delay diversity
CDF	Cumulative distribution function
CDL	Clustered delay line
ChIR	Channel impulse response
<i>C/I</i>	Carrier-to-interference
CRC	Cyclic redundancy code
DL	Down link
DS	Delay spread
FDD	Frequency division duplex
HARQ	Hybrid automatic repeat request
HH	Horizontal-to-horizontal
HV	Horizontal-to-vertical
InH	Indoor hotspot
IoT	Interference over thermal
IP	Internet protocol
ISD	Inter-site distance
LN	Log-normal
LoS	Line of sight
LS	Large scale
MAC	Media access control
MIMO	Multiple input multiple output
NACK	Negative acknowledgment
NLoS	Non line-of-sight
OSI	Open systems interconnection
PAS	Power angular spectrum
PDP	Power delay profile
PDU	Protocol data unit
PL	Path loss
RF	Radio frequency
RIT	Radio interface technology
RMa	Rural macro
RMS	Root mean square (alias: rms)

RRC	Radio resource controller
RRM	Radio resource management
RTP	Real-time transport protocol
RX	Receive (alias: Rx, rx)
SCM	Spatial channel model
SF	Shadow fading
SMa	Suburban macro
SRIT	Set of radio interface technologies
SS	Small scale
TDD	Time division duplex
TDL	Tapped delay line
TSP	Time-spatial propagation
TTI	Transmission time interval
TX	Transmit (alias: Tx, tx)
UDP	User datagram protocol
UL	Up link
ULA	Uniform linear arrays
UMa	Urban macro
UMi	Urban micro
UT	User terminal
VAF	Voice activity factor
VoIP	Voice over IP
VH	Vertical-to-horizontal
VV	Vertical-to-vertical
XPD	Cross-polarization discrimination
XPR	Cross-polarization ratio

Further information on vocabulary can be found in the references at the bottom of the page^{*, **, ***}.

References

STEINBAUER, M., MOLISCH, A. F. and BONEK, E. [August 2001] The double-directional radio channel. *IEEE Ant. Prop. Mag.*, p. 51-63.

* 3GPP TR 21.905 Vocabulary For 3GPP Specifications (<http://www.3gpp.org/ftp/Specs/html-info/21905.htm>).

** IEEE 802.16e-2005 (Definitions Section 3) (<http://standards.ieee.org/getieee802/download/802.16e-2005.pdf>).

*** 3GPP2 UMB PHY Specification Ver.2.0 (Terms Section 2.1) (http://www.3gpp2.org/Public_html/specs/C.S0084-001-0_v2.0_070904.pdf).

Annex 1

Test environments and channel models

1 Test environments and channel models

This section provides the reference channel model for each test environment. These test environments are intended to cover the range of IMT-Advanced operating environments.

The test operating environments are considered as a basic factor in the evaluation process of the candidate RITs. The reference models are used to estimate the critical aspects, such as the spectrum, coverage and power efficiencies.

1.1 Test environments, deployment scenarios and network layout

Evaluation of candidate IMT-Advanced RIT/SRITs will be performed in selected scenarios of the following test environments:

- **Base coverage urban:** an urban macro-cellular environment targeting continuous coverage for pedestrian up to fast vehicular users.
- **Micro-cellular:** an urban micro-cellular environment with higher user density focusing on pedestrian and slow vehicular users.
- **Indoor:** an indoor environment targeting isolated cells at offices and/or in hotspot based on stationary and pedestrian users.
- **High speed:** a macro-cellular environment with high speed vehicles and trains.

The deployment scenarios that shall be used for each test environment are shown in Table 8-1; information of the respective channel models is given in Table A1-1.

TABLE A1-1

Selected deployment scenarios for evaluation and the channel models

Test environment	Base coverage urban	Microcellular	Indoor	High speed
Deployment scenario	Urban macro-cell scenario	Urban micro-cell scenario	Indoor hotspot scenario	Rural macro-cell scenario
Channel model	UMa Urban macro (LoS, NLoS)	UMi Urban micro (LoS, NLoS, Outdoor-to-indoor)	InH Indoor hotspot (LoS, NLoS)	RMa Rural macro (LoS, NLoS)

Suburban macro-cell scenario (and corresponding SMA channel model) is an optional scenario for the base coverage urban test environment.

Initial focus for deployment and most challenges in IMT-Advanced system design and performance will be encountered in populated areas. However, in the evaluation the provisions for ubiquitous coverage and the associated performance also in rural areas need to be addressed.

1.2 Test environments

For evaluation of candidate IMT-Advanced RIT/SRITs in the four selected test environments, a set of reliable and measurement-based channel models are needed. Channel models have to be accurate due to the fact that radio propagation has a significant impact on the performance of future broadband systems. This is especially true with future multiple-input multiple-output (MIMO) radio

communication systems since more of the radio channel degrees of freedom in space, time, frequency, and polarization may be exploited to meet the demands on bit rate, spectrum efficiency, and cost. Channel models are needed in performance evaluation of wireless systems when choosing modulation and coding, in multi antenna system design, in the selection of channel estimation method, channel equalization and other baseband algorithm design, as well as network planning. It is important to use common and uniform channel models for evaluation, comparison, and selection of technologies. In this context it is clear that realistic and reliable multidimensional channel models are an important part of the performance evaluation of IMT-Advanced RIT/SRITs.

A central factor of mobile radio propagation environments is the multi-path propagation causing frequency and time dispersion as well as angular dispersion in Tx and Rx. The fading characteristics vary with the propagation environment and their impact on the communication quality (e.g., bit error patterns) highly depends on the speed of the mobile station relative to the serving base station.

The purpose of the test environments is to challenge the RITs. Instead of constructing propagation models for all the possible IMT-Advanced operating environments, a smaller set of test environments is defined which adequately span the overall range of possible environments. The descriptions of these test environments may therefore not correspond with those of the actual operating environments.

This section identifies the propagation and channel model for each test operating environment described in § 1.2.1 to 1.2.4. For practical reasons, these test operating environments are an appropriate subset of the IMT-Advanced operating environments. While simple models might be adequate to evaluate the performance of individual radio links, more complex models are needed to evaluate the overall system-level reliability and suitability of specific technologies. For wideband technologies the number, strength, and relative time delay as well as the directions at Tx and Rx of the many signal components become important. For some technologies (e.g., those employing power control) these models must include coupling between all co-channel propagation links to achieve maximum accuracy. Also, in some cases, the large-scale (shadow fading) temporal variations of the environment must be modelled.

The key parameters to describe channel models include, e.g., delay spread, angle spread, path loss, etc.

1.2.1 Base coverage urban test environment

The base coverage urban test environment focuses on large cells and continuous coverage. The key characteristics of this test environment are continuous and ubiquitous coverage in urban areas. This scenario will therefore be interference-limited, using macro cells (i.e. radio access points above rooftop level).

In urban macro-cell scenario mobile station is located outdoors at street level and fixed base station antenna clearly above surrounding building heights. As for propagation conditions, non- or obstructed line-of-sight is a common case, since street level is often reached by a single diffraction over the rooftop. The building blocks can form either a regular Manhattan type of grid, or have more irregular locations. Typical building heights in urban environments are over four floors. Buildings height and density in typical urban macro-cell are mostly homogenous.

The base coverage urban test environment is intended to prove that continuous, ubiquitous, and cost-effective coverage in built-up areas is feasible in the IMT-Advanced bands by the candidate IMT-Advanced RIT/SRITs. This scenario will therefore be interference-limited, using macro cells (i.e., radio access points above rooftop level) and still assume that the users require access to demanding services beyond baseline voice and text messages.

1.2.1.1 Urban macro-cell scenario

In typical urban macro-cell scenario, the mobile station is located outdoors at street level and the fixed base station clearly above the surrounding building heights. As for propagation conditions, non- or obstructed line-of-sight are common cases, since street level is often reached by a single diffraction over the rooftop. The building blocks can form either a regular Manhattan type of grid, or have more irregular locations. Typical building heights in urban environments are over four floors. Buildings height and density in typical urban macro-cell are mostly homogenous.

The channel model for urban macro-cell scenario is called urban macro (UMa).

1.2.1.2 Suburban macro-cell scenario (Optional)

In suburban macro-cell scenario base stations are located well above the rooftops to allow wide area coverage, and mobile stations are outdoors at street level. Buildings are typically low residential detached houses with one or two floors, or blocks of flats with a few floors. Occasional open areas such as parks or playgrounds between the houses make the environment rather open. Streets do not form urban-like regular strict grid structure. Vegetation is modest.

The channel model for suburban macro-cell scenario is called suburban macro (SMa).

1.2.2 Microcellular test environment

The microcellular test environment focuses on small cells and high user densities and traffic loads in city centres and dense urban areas. The key characteristics of this test environment are high traffic loads, outdoor and outdoor-to-indoor coverage. This scenario will therefore be interference-limited, using micro cells. A continuous cellular layout and the associated interference shall be assumed. Radio access points shall be below rooftop level.

A similar scenario is used to the base coverage urban test environment but with reduced site-to-site distance and the antennas below rooftops.

The microcellular test environment focuses on smaller cells and higher user densities and traffic loads in city centres and dense urban areas, i.e., it targets the high-performance layer of an IMT-Advanced system in metropolitan areas. It is thus intended to test the performance in high traffic loads and using demanding user requirements, including detailed modelling of buildings (e.g., Manhattan grid deployment) and outdoor-to-indoor coverage. A continuous cellular layout and the associated interference shall be assumed. Radio access points shall be below rooftop level.

1.2.2.1 Urban micro-cell scenario

In urban micro-cell scenario the height of both the antenna at the BS and that at the UT is assumed to be well below the tops of surrounding buildings. Both antennas are assumed to be outdoors in an area where streets are laid out in a Manhattan-like grid. The streets in the coverage area are classified as “the main street”, where there is LoS from all locations to the BS, with the possible exception of cases in which LoS is temporarily blocked by traffic (e.g., trucks and busses) on the street. Streets that intersect the main street are referred to as perpendicular streets, and those that run parallel to it are referred to as parallel streets. This scenario is defined for both LoS and NLoS cases. Cell shapes are defined by the surrounding buildings, and energy reaches NLoS streets as a result of propagation around corners, through buildings, and between them.

The microcellular test environment includes outdoor and outdoor-to-indoor users: In the latter case the users are located indoors and Base Stations outdoors. Therefore the channel model for the micro-cellular test environment contains two parts, the outdoor part and the outdoor-to-indoor part.

The channel model for urban micro-cell scenario is called urban micro (UMi).

1.2.3 Indoor test environment

The indoor test environment focuses on smallest cells and high user throughput in buildings. The key characteristics of this test environment are high user throughput in indoor coverage.

1.2.3.1 Indoor hotspot scenario

The indoor hotspot scenario consists of one floor of a building. The height of the floor is 6 m. The floor contains 16 rooms of 15 m × 15 m and a long hall of 120 m × 20 m. Two sites are placed in the middle of the hall at 30 m and 90 m with respect to the left side of the building (see Fig. 2).

The channel model for indoor hotspot scenario is called indoor hotspot (InH).

1.2.4 High-speed test environment

The high-speed test environment focuses on larger cells and continuous coverage. The key characteristics of this test environment are continuous wide area coverage supporting high speed vehicles. This scenario will therefore be noise-limited and/or interference-limited, using macro cells.

The high speed test environment is applicable to a wide-area system concept since it should allow for reliable links to high-speed trains of up to 350 km/h or cars at high velocities. Repeater technology or relays (relaying to the same wide area system, IMT-2000, or to a local area system) can be applied in the vehicle, to allow for local access by the users.

1.2.4.1 Rural macro-cell scenario

The Rural macro-cell scenario propagation scenario represents radio propagation in large areas (radii up to 10 km) with low building density. The height of the BS antenna is typically in the range from 20 to 70 m, which is much higher than the average building height. Consequently, LoS conditions can be expected to exist in most of the coverage area. In case the UT is located inside a building or vehicle, an additional penetration loss is experienced which can possibly be modelled as a (frequency-dependent) constant value. The BS antenna location is fixed in this propagation scenario, and the UT antenna velocity is in the range from 0 to 350 km/h.

The channel model for rural macro-cell scenario is called rural macro (RMa).

1.2.5 Simulation of relays

It is possible to simulate relay-based lay-outs with the proposed channel models by using models for the constituent hops of the multiple links. The link from a relay to a mobile station can be modeled with the same models as the conventional link from a base station to a mobile station. The links from base stations to relay stations can be modeled with conventional links.

1.3 Primary module

The following sections provide the details of the channel models, including the path loss models, for the terrestrial component. For terrestrial environments, the propagation effects are divided into three distinct types: These are the path loss, the slow variation due to shadowing and scattering, and the rapid variation in the signal due to multipath effects. The channel models are specified in the frequency range from 2 GHz to 6 GHz. For the rural macro-cell scenario (RMa), the channel model can be used for lower frequencies down to 450 MHz. The channel models also cover MIMO aspects as all desired dimensions (delay, AoA, AoD and polarisation) are considered. The channel models are targeted for up to 100 MHz RF bandwidth.

1.3.1 Path loss models

Path loss models for the various propagation scenarios have been developed based on measurement results carried out in references* [Dong *et al.*, 2007; Fujii, 2003; Lu *et al.*, 2007; Xinying *et al.*, 2007; Xu *et al.*, 2007; Zhang *et al.*, 2007 and 2008], as well as results from the literature. The models can be applied in the frequency range of 2-6 GHz and for different antenna heights. The rural path-loss formula can be applied to the desired frequency range from 450 MHz to 6 GHz. The path loss models have been summarized in Table A1-2. Note that the distribution of the shadow fading is log-normal, and its standard deviation for each scenario is given in the following table.

TABLE A1-2

Summary table of the primary module path loss models

Scenario	Path loss (dB) <i>Note: f_c is given in GHz and distance in m!</i>	Shadow fading std (dB)	Applicability range, antenna height default values
Indoor Hotspot (InH)	LoS $PL = 16.9 \log_{10}(d) + 32.8 + 20 \log_{10}(f_c)$	$\sigma = 3$	$3 \text{ m} < d < 100 \text{ m}$ $h_{BS} = 3\text{-}6 \text{ m}$ $h_{UT} = 1\text{-}2.5 \text{ m}$
	NLoS $PL = 43.3 \log_{10}(d) + 11.5 + 20 \log_{10}(f_c)$	$\sigma = 4$	$10 \text{ m} < d < 150 \text{ m}$ $h_{BS} = 3\text{-}6 \text{ m}$ $h_{UT} = 1\text{-}2.5 \text{ m}$
Urban Micro (UMi)	LoS $PL = 22.0 \log_{10}(d) + 28.0 + 20 \log_{10}(f_c)$	$\sigma = 3$	$10 \text{ m} < d_1 < d'_{BP} \text{ }^{(1)}$
	LoS $PL = 40 \log_{10}(d_l) + 7.8 - 18 \log_{10}(h'_{BS}) - 18 \log_{10}(h'_{UT}) + 2 \log_{10}(f_c)$	$\sigma = 3$	$d'_{BP} < d_1 < 5 \text{ 000 m} \text{ }^{(1)}$ $h_{BS} = 10 \text{ m} \text{ }^{(1)}$, $h_{UT} = 1.5 \text{ m} \text{ }^{(1)}$
	NLoS Manhattan grid layout: $PL = \min(PL(d_1, d_2), PL(d_2, d_1))$ where: $PL(d_k, d_l) = PL_{LOS}(d_k) + 17.9 - 12.5n_j + 10n_j \log_{10}(d_l) + 3 \log_{10}(f_c)$ and $n_j = \max(2.8 - 0.0024d_k, 1.84)$ PL_{LOS} : path loss of scenario UMi LoS and $k, l \in \{1, 2\}$. Hexagonal cell layout: $PL = 36.7 \log_{10}(d) + 22.7 + 26 \log_{10}(f_c)$	$\sigma = 4$	$10 \text{ m} < d_1 + d_2 < 5 \text{ 000 m}$, $w/2 < \min(d_1, d_2) \text{ }^{(2)}$ $w = 20 \text{ m}$ (street width) $h'_{BS} = 10 \text{ m}$, $h_{UT} = 1.5 \text{ m}$. When $0 < \min(d_1, d_2) < w/2$, the LoS PL is applied.
O-to-I $PL = PL_b + PL_{tw} + PL_{in}$ Manhattan grid layout (θ known): $\begin{cases} PL_b = PL_{B1}(d_{out} + d_{in}) \\ PL_{tw} = 14 + 15(1 - \cos(\theta))^2 \\ PL_{in} = 0.5d_{in} \end{cases}$ For hexagonal layout (θ unknown): $PL_{tw} = 20$, other values remain the same.	$\sigma = 7$	$10 \text{ m} < d_{out} + d_{in} < 1 \text{ 000 m}$, $0 \text{ m} < d_{in} < 25 \text{ m}$, $h_{BS} = 10 \text{ m}$, $h_{UT} = 3(n_{FI} - 1) + 1.5 \text{ m}$, $n_{FI} = 1$ <i>Explanations: see</i> ⁽³⁾	

* IST-WINNER II Deliverable 1.1.2 v.1.2. WINNER II Channel Models, IST-WINNER2, Tech. Rep., 2008 (<http://www.ist-winner.org/deliverables.html>).

TABLE A1-2 (end)

Scenario	Path loss (dB) <i>Note: f_c is given in GHz and distance in m!</i>	Shadow fading std (dB)	Applicability range, antenna height default values
Urban Macro (UMa)	LoS $PL = 22.0 \log_{10}(d) + 28.0 + 20 \log_{10}(f_c)$	$\sigma = 4$	$10 \text{ m} < d < d'_{BP} \text{ }^{(1)}$
	NLoS $PL = 40.0 \log_{10}(d_1) + 7.8 - 18.0 \log_{10}(h'_{BS}) - 18.0 \log_{10}(h'_{UT}) + 2.0 \log_{10}(f_c)$	$\sigma = 4$	$d'_{BP} < d < 5\,000 \text{ m} \text{ }^{(1)}$ $h_{BS} = 25 \text{ m} \text{ }^{(1)}, h_{UT} = 1.5 \text{ m} \text{ }^{(1)}$
	$PL = 161.04 - 7.1 \log_{10}(W) + 7.5 \log_{10}(h) - (24.37 - 3.7(h/h_{BS})^2) \log_{10}(h_{BS}) + (43.42 - 3.1 \log_{10}(h_{BS})) (\log_{10}(d) - 3) + 20 \log_{10}(f_c) - (3.2 (\log_{10}(11.75 h_{UT}))^2 - 4.97)$	$\sigma = 6$	$10 \text{ m} < d < 5\,000 \text{ m}$ $h = \text{avg. building height}$ $W = \text{street width}$ $h_{BS} = 25 \text{ m}, h_{UT} = 1.5 \text{ m},$ $W = 20 \text{ m}, h = 20 \text{ m.}$ The applicability ranges: $5 \text{ m} < h < 50 \text{ m}$ $5 \text{ m} < W < 50 \text{ m}$ $10 \text{ m} < h_{BS} < 150 \text{ m}$ $1 \text{ m} < h_{UT} < 10 \text{ m}$
Suburban Macro (SMa, optional)	LoS $PL_1 = 20 \log_{10}(40\pi d f_c/3) + \min(0.03h^{1.72}, 10) \log_{10}(d) - \min(0.044h^{1.72}, 14.77) + 0.002 \log_{10}(h)d$ $PL_2 = PL_1(d_{BP}) + 40 \log_{10}(d/d_{BP})$	$\sigma = 4$ $\sigma = 6$	$10 \text{ m} < d < d_{BP} \text{ }^{(4)}$ $d_{BP} < d < 5\,000 \text{ m}$ $h_{BS} = 35 \text{ m}, h_{UT} = 1.5 \text{ m},$ $W = 20 \text{ m}, h = 10 \text{ m}$ (The applicability ranges of h, W, h_{BS}, h_{UT} are same as in UMa NLoS)
	NLoS $PL = 161.04 - 7.1 \log_{10}(W) + 7.5 \log_{10}(h) - (24.37 - 3.7(h/h_{BS})^2) \log_{10}(h_{BS}) + (43.42 - 3.1 \log_{10}(h_{BS})) (\log_{10}(d) - 3) + 20 \log_{10}(f_c) - (3.2 (\log_{10}(11.75 h_{UT}))^2 - 4.97)$	$\sigma = 8$	$10 \text{ m} < d < 5\,000 \text{ m}$ $h_{BS} = 35 \text{ m}, h_{UT} = 1.5 \text{ m},$ $W = 20 \text{ m}, h = 10 \text{ m}$ (Applicability ranges of h, W, h_{BS}, h_{UT} are same as in UMa NLoS)
Rural Macro (RMa)	LoS $PL_1 = 20 \log_{10}(40\pi d f_c/3) + \min(0.03h^{1.72}, 10) \log_{10}(d) - \min(0.044h^{1.72}, 14.77) + 0.002 \log_{10}(h)d$ $PL_2 = PL_1(d_{BP}) + 40 \log_{10}(d/d_{BP})$	$\sigma = 4$ $\sigma = 6$	$10 \text{ m} < d < d_{BP} \text{ }^{(4)}$ $d_{BP} < d < 10\,000 \text{ m},$ $h_{BS} = 35 \text{ m}, h_{UT} = 1.5 \text{ m},$ $W = 20 \text{ m}, h = 5 \text{ m}$ (Applicability ranges of h, W, h_{BS}, h_{UT} are same as UMa NLoS)
	NLoS $PL = 161.04 - 7.1 \log_{10}(W) + 7.5 \log_{10}(h) - (24.37 - 3.7(h/h_{BS})^2) \log_{10}(h_{BS}) + (43.42 - 3.1 \log_{10}(h_{BS})) (\log_{10}(d) - 3) + 20 \log_{10}(f_c) - (3.2 (\log_{10}(11.75 h_{UT}))^2 - 4.97)$	$\sigma = 8$	$10 \text{ m} < d < 5\,000 \text{ m},$ $h_{BS} = 35 \text{ m}, h_{UT} = 1.5 \text{ m},$ $W = 20 \text{ m}, h = 5 \text{ m}$ (The applicability ranges of h, W, h_{BS}, h_{UT} are same as UMa NLoS)

Notes to Table A1-2:

- (1) Break point distance $d'_{BP} = 4 h'_{BS} h'_{UT} f_c / c$, where f_c is the centre frequency (Hz), $c = 3.0 \times 10^8$ m/s is the propagation velocity in free space, and h'_{BS} and h'_{UT} are the effective antenna heights at the BS and the UT, respectively. The effective antenna heights h'_{BS} and h'_{UT} are computed as follows:

$$h'_{BS} = h_{BS} - 1.0 \text{ m}, h'_{UT} = h_{UT} - 1.0 \text{ m}$$

where: h_{BS} and h_{UT} are the actual antenna heights, and the effective environment height in urban environments is assumed to be equal to 1.0 m.

- (2) The distances d_1 and d_2 are defined below in Fig. 12.
- (3) PL_b : basic path-loss, PL_{BJ} : loss of UMi outdoor scenario, PL_{tw} : loss through wall, PL_{in} : loss inside, d_{out} : distance from BS to the wall next to UT location, d_{in} : perpendicular distance from wall to UT (assumed evenly distributed between 0 and 25 m), θ : angle between LoS to the wall and a unit vector normal to the wall.
- (4) Break point distance $d_{BP} = 2\pi h_{BS} h_{UT} f_c / c$, where f_c is the centre frequency in Hz, $c = 3.0 \times 10^8$ m/s is the propagation velocity in free space, and h_{BS} and h_{UT} are the antenna heights at the BS and the UT, respectively.

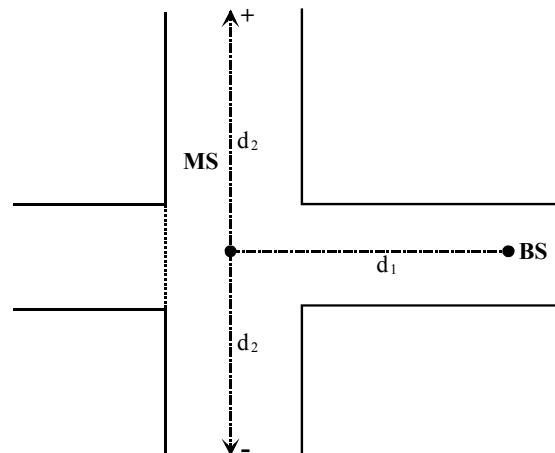
The LoS probabilities are given in Table A1-3. Note that probabilities are used only for system level simulations.

TABLE A1-3

Scenario	LoS probability as a function of distance, d (m)
InH	$P_{LOS} = \begin{cases} 1, & d \leq 18 \\ \exp(-(d-18)/27), & 18 < d < 37 \\ 0.5, & d \geq 37 \end{cases}$
UMi	$P_{LOS} = \min(18/d, 1) \cdot (1 - \exp(-d/36)) + \exp(-d/36)$ (for outdoor users only)
UMa	$P_{LOS} = \min(18/d, 1) \cdot (1 - \exp(-d/63)) + \exp(-d/63)$
SMa	$P_{LOS} = \begin{cases} 1, & d \leq 10 \\ \exp(-(d-10)/200), & d > 10 \end{cases}$
RMa	$P_{LOS} = \begin{cases} 1, & d \leq 10 \\ \exp\left(-\frac{d-10}{1000}\right), & d > 10 \end{cases}$

The NLoS path loss model for scenario UMi is dependent on two distances, d_1 and d_2 in the case of the Manhattan grid. These distances are defined with respect to a rectangular street grid, as illustrated in Fig. 12, where the UT is shown moving along a street perpendicular to the street on which the BS is located (the LoS street). d_1 is the distance from the BS to the centre of the perpendicular street, and d_2 is the distance of the UT along the perpendicular street, measured from the centre of the LoS street.

FIGURE 8
Geometry for $d_1 - d_2$ path-loss model



1.3.1.1 Autocorrelation of shadow fading

The long-term (log-normal) fading in the logarithmic scale around the mean path loss PL (dB) is characterized by a Gaussian distribution with zero mean and standard deviation. Due to the slow fading process versus distance Δx , adjacent fading values are correlated. Its normalized autocorrelation function $R(\Delta x)$ can be described with sufficient accuracy by the exponential function (Recommendation ITU-R P.1816 – The prediction of the time and the spatial profile for broadband land mobile services using UHF and SHF bands):

$$R(\Delta x) = e^{-\frac{|\Delta x|}{d_{cor}}} \quad (6)$$

with the correlation length d_{cor} being dependent on the environment, see the correlation parameters for shadowing and other large scale parameters in Table A1-7.

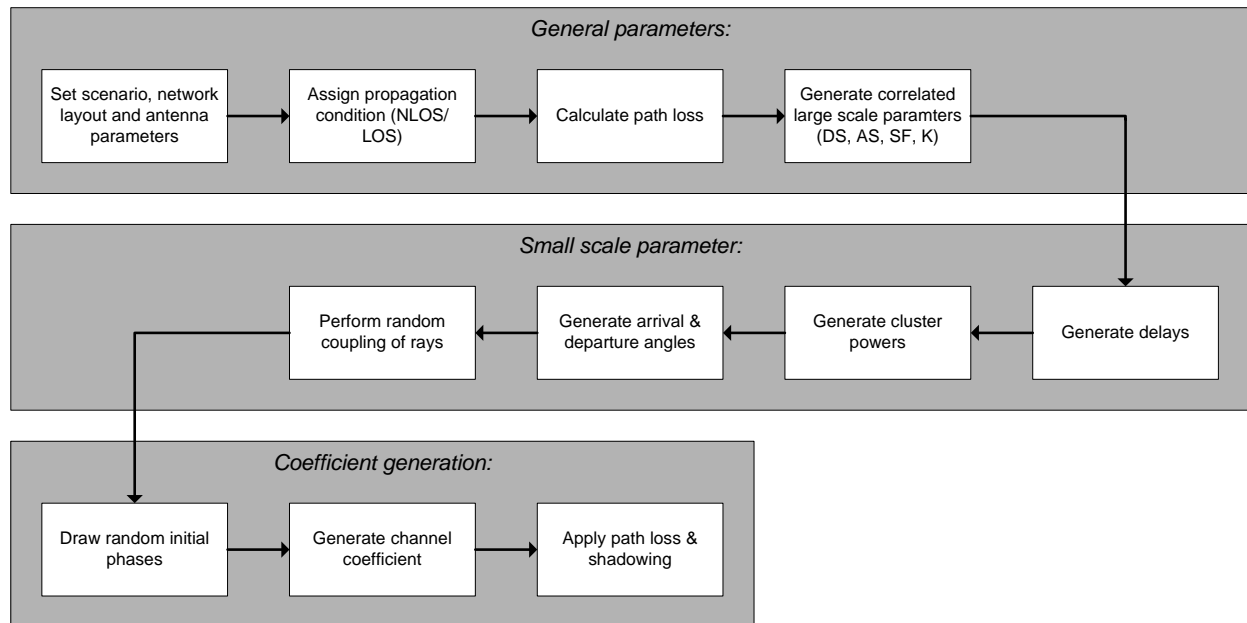
1.3.2 Primary module channel model parameters

1.3.2.1 Generic model

The radio channels are created using the parameters listed in Table A1-7. The channel realizations are obtained by a step-wise procedure* illustrated in Fig. 9 and described below. It has to be noted that the geometric description covers arrival angles from the last bounce scatterers and respectively departure angles to the first scatterers interacted from the transmitting side. The propagation between the first and the last interaction is not defined. Thus, this approach can model also multiple interactions with the scattering media. This indicates also that e.g., the delay of a multipath component cannot be determined by the geometry. In the following steps, downlink is assumed. For uplink, arrival and departure parameters have to be swapped.

* IST-WINNER II Deliverable 1.1.2 v.1.2. WINNER II Channel Models, IST-WINNER2. Tech. Rep., 2008 (<http://www.ist-winner.org/deliverables.html>).

FIGURE 9
Channel coefficient generation procedure



General parameters:

Step 1: Set environment, network layout, and antenna array parameters:

- Choose one of the scenarios (InH, UMi, ...)
- Give number of BS and UT
- Give locations of BS and UT, or equally distances of each BS and UT and relative directions and ϕ_{LoS} and φ_{LoS} of each BS and UT
- Give BS and UT antenna field patterns F_{rx} and F_{tx} and array geometries
- Give BS and UT array orientations with respect to north (reference) direction
- Give speed and direction of motion of UT
- Give system centre frequency.

Large scale parameters:

Step 2: Assign propagation condition (LoS/NLoS).

Step 3: Calculate path loss with formulas of Table A1-2 for each BS-UT link to be modelled.

Step 4: Generate correlated large scale parameters, i.e. delay spread, angular spreads, Ricean K factor and shadow fading term like explained in § 3.3.1 (Correlations between large scale parameters) of reference*. Limit random rms arrival and departure azimuth spread values to 104° , i.e., $\sigma_\varphi = \min(\sigma_\varphi, 104^\circ)$.

* IST-WINNER II Deliverable 1.1.2 v.1.2. WINNER II Channel Models, IST-WINNER2. Tech. Rep., 2008 (<http://www.ist-winner.org/deliverables.html>).

Small scale parameters:

Step 5: Generate delays τ .

Delays are drawn randomly from the delay distribution defined in Table A1-7. With exponential delay distribution calculate:

$$\tau_n' = -r_\tau \sigma_\tau \ln(X_n) \quad (7)$$

where r_τ is the delay distribution proportionality factor, $X_n \sim \text{Uni}(0,1)$, and cluster index $n = 1, \dots, N$. With uniform delay distribution the delay values τ_n' are drawn from the corresponding range. Normalise the delays by subtracting the minimum delay and sort the normalised delays to descending order:

$$\tau_n = \text{sort}(\tau_n' - \min(\tau_n')). \quad (8)$$

In the case of LoS condition, additional scaling of delays is required to compensate for the effect of LoS peak addition to the delay spread. The heuristically determined Ricean K -factor dependent scaling constant is:

$$D = 0.7705 - 0.0433K + 0.0002K^2 + 0.000017K^3 \quad (9)$$

where K (dB) is the Ricean K -factor defined in Table A1-7. The scaled delays:

$$\tau_n^{LoS} = \tau_n / D \quad (10)$$

are **not** to be used in cluster power generation.

Step 6: Generate cluster powers, P .

Cluster powers are calculated assuming a single slope exponential power delay profile. Power assignment depends on the delay distribution defined in Table A1-7. With exponential delay distribution the cluster powers are determined by:

$$P_n' = \exp\left(-\tau_n \frac{r_\tau - 1}{r_\tau \sigma_\tau}\right) \cdot 10^{\frac{-Z_n}{10}} \quad (11)$$

where $Z_n \sim N(0, \zeta)$ is the per cluster shadowing term (dB). Average the power so that the sum power of all cluster powers is equal to one, i.e.:

$$P_n = \frac{P_n'}{\sum_{n=1}^N P_n'} \quad (12)$$

Assign the power of each ray within a cluster as P_n/M , where M is the number of rays per cluster.

Remove clusters with less than -25 dB power compared to the maximum cluster power.

Step 7: Generate arrival angles φ and departure angles ϕ .

As the composite PAS of all clusters is modelled as wrapped Gaussian (see Table A1-7), except indoor hotspot scenario (InH) as Laplacian, the AoAs are determined by applying the inverse Gaussian function (13) or inverse Laplacian function (14) with input parameters P_n and RMS angle spread σ_φ :

$$\varphi_n' = \frac{2\sigma_{AoA} \sqrt{-\ln(P_n / \max(P_n))}}{C} \quad (13)$$

$$\varphi_n' = -\frac{\sigma_\varphi \ln(P_n / \max(P_n))}{C} \quad (14)$$

In equation (13), $\sigma_{AoA} = \sigma_\varphi / 1.4$ is the standard deviation of the arrival angles (the factor 1.4 is the ratio of Gaussian std and the corresponding ‘‘RMS spread’’). Constant C is a scaling factor related to total number of clusters and is given in Table A1-4:

TABLE A1-4

No. clusters	4	5	8	10	11	12	14	15	15 (lnH)	16	19	19 (lnH)	20
C	0.779	0.860	1.018	1.090	1.123	1.146	1.190	1.211	1.434	1.226	1.273	1.501	1.289

In the LoS case, constant C is dependent also on the Ricean K -factor. Constant C in equations (13) and (14) is substituted by C^{LoS} . Additional scaling of the angles is required to compensate for the effect of LOS peak addition to the angle spread. The heuristically determined Ricean K -factor dependent scaling constant is:

$$C^{LoS} = C \cdot (1.1035 - 0.028K - 0.002K^2 + 0.0001K^3) \quad (15)$$

As for indoor hotspot scenario, the scaling constant is:

$$C^{LoS} = C \cdot (0.9275 + 0.0439K - 0.0071K^2 + 0.0002K^3) \quad (16)$$

where K (dB) is the Ricean K -factor defined in Table A1-7.

Assign positive or negative sign to the angles by multiplying with a random variable X_n with uniform distribution to the discrete set of $\{1, -1\}$, and add component $Y_n \sim N(0, \sigma_\varphi / 7)$ to introduce random variation:

$$\varphi_n = X_n \varphi_n' + Y_n + \varphi_{LoS} \quad (17)$$

where φ_{LoS} is the LoS direction defined in the network layout description, see Step 1c).

In the LoS case, substitute equation (17) by equation (18) to enforce the first cluster to the LoS direction φ_{LoS} :

$$\varphi_n = (X_n \varphi_n' + Y_n) - (X_1 \varphi_1' + Y_1 - \varphi_{LoS}) \quad (18)$$

Finally add offset angles α_m from Table A1-5 to the cluster angles:

$$\varphi_{n,m} = \varphi_n + c_{AoA} \alpha_m \quad (19)$$

where c_{AoA} is the cluster-wise rms azimuth spread of arrival angles (cluster ASA) in Table A1-7.

TABLE A1-5

Ray offset angles within a cluster, given
for 1 rms angle spread

Ray number, m	Basis vector of offset angles, α_m
1,2	± 0.0447
3,4	± 0.1413
5,6	± 0.2492
7,8	± 0.3715
9,10	± 0.5129
11,12	± 0.6797
13,14	± 0.8844
15,16	± 1.1481
17,18	± 1.5195
19,20	± 2.1551

For departure angles ϕ_n the procedure is similar.

Step 8: Random coupling of rays within clusters.

Couple randomly departure ray angles $\phi_{n,m}$ to arrival ray angles $\phi_{n,m}$ within a cluster n , or within a sub-cluster in the case of two strongest clusters (see Step 10a and Table A1-5).

Coefficient generation:

Step 9: Draw random initial phase $\{\Phi_{n,m}^{vv}, \Phi_{n,m}^{vh}, \Phi_{n,m}^{hv}, \Phi_{n,m}^{hh}\}$ for each ray m of each cluster n and for four different polarisation combinations (vv, vh, hv, hh). The distribution for initial phases is uniform within $(-\pi, \pi)$.

In the LoS case, draw also random initial phases $\{\Phi_{LOS}^{vv}, \Phi_{LOS}^{hh}\}$ for both VV and HH polarisations.

Step 10a: Generate channel coefficients for each cluster n and each receiver and transmitter element pair u, s .

For the $N - 2$ weakest clusters, say $n = 3, 4, \dots, N$, and uniform linear arrays (ULA), the channel coefficients are given by:

$$\mathbf{H}_{u,s,n}(t) = \sqrt{P_n} \sum_{m=1}^M \begin{bmatrix} F_{rx,u,V}(\phi_{n,m}) \\ F_{rx,u,H}(\phi_{n,m}) \end{bmatrix}^T \begin{bmatrix} \exp(j\Phi_{n,m}^{vv}) & \sqrt{\kappa^{-1}} \exp(j\Phi_{n,m}^{vh}) \\ \sqrt{\kappa^{-1}} \exp(j\Phi_{n,m}^{hv}) & \exp(j\Phi_{n,m}^{hh}) \end{bmatrix} \begin{bmatrix} F_{tx,s,V}(\phi_{n,m}) \\ F_{tx,s,H}(\phi_{n,m}) \end{bmatrix} \cdot \exp(jd_s 2\pi\lambda_0^{-1} \sin(\phi_{n,m})) \exp(jd_u 2\pi\lambda_0^{-1} \sin(\phi_{n,m})) \exp(j2\pi\nu_{n,m}t) \quad (20)$$

where $F_{rx,u,V}$ and $F_{rx,u,H}$ are the antenna element, u , field patterns for vertical and horizontal polarisations respectively, d_s and d_u are the uniform distances (m) between transmitter elements and receiver elements respectively, κ is the cross polarisation power ratio in linear scale, and λ_0 is the wavelength of the carrier frequency. If polarisation is not considered, the 2×2 polarisation matrix can be replaced by the scalar $\exp(j\Phi_{n,m})$ and only vertically polarised field patterns are applied.

The Doppler frequency component is calculated from the angle of arrival (downlink), UT speed v and direction of travel θ_v :

$$v_{n,m} = \frac{\|v\| \cos(\varphi_{n,m} - \theta_v)}{\lambda_0} \quad (21)$$

For the two strongest clusters, say $n = 1$ and 2, rays are spread in delay to three sub-clusters (per cluster), with fixed delay offset $\{0, 5, 10\}$ ns (see Table A1-6). The delays of the sub-clusters are:

$$\begin{aligned} \tau_{n,1} &= \tau_n + 0 \text{ ns} \\ \tau_{n,2} &= \tau_n + 5 \text{ ns} \\ \tau_{n,3} &= \tau_n + 10 \text{ ns} \end{aligned} \quad (22)$$

Twenty rays of a cluster are mapped to sub-clusters as presented in Table A1-6. The corresponding offset angles are taken from Table A1-5 with mapping of Table A1-6.

TABLE A1-6
Sub-cluster information for intra cluster
delay spread clusters

Sub-cluster No.	Mapping to rays	Power	Delay offset
1	1, 2, 3, 4, 5, 6, 7, 8, 19, 20	10/20	0 ns
2	9, 10, 11, 12, 17, 18	6/20	5 ns
3	13, 14, 15, 16	4/20	10 ns

In the LoS case, define $\mathbf{H}'_{u,s,n} = \mathbf{H}_{u,s,n}$ and determine the channel coefficients by adding a single line-of-sight ray and scaling down the other channel coefficient generated by equation (20). The channel coefficients are given by:

$$\begin{aligned} \mathbf{H}_{u,s,n}(t) &= \sqrt{\frac{1}{K_R + 1}} \mathbf{H}'_{u,s,n}(t) \\ &+ \delta(n-1) \sqrt{\frac{K_R}{K_R + 1}} \begin{bmatrix} F_{rx,u,V}(\varphi_{LOS}) \\ F_{rx,u,H}(\varphi_{LOS}) \end{bmatrix}^T \begin{bmatrix} \exp(j\Phi_{LOS}^{vv}) & 0 \\ 0 & \exp(j\Phi_{LOS}^{hh}) \end{bmatrix} \begin{bmatrix} F_{tx,s,V}(\varphi_{LOS}) \\ F_{tx,s,H}(\varphi_{LOS}) \end{bmatrix} \\ &\cdot \exp(jd_s 2\pi\lambda_0^{-1} \sin(\varphi_{LOS})) \exp(jd_u 2\pi\lambda_0^{-1} \sin(\varphi_{LOS})) \exp(j2\pi v_{LOS} t) \end{aligned} \quad (23)$$

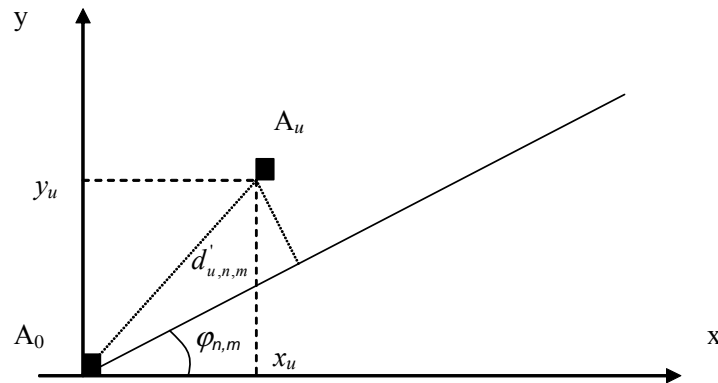
where $\delta(\cdot)$ is the Dirac's delta function and K_R is the Ricean K -factor defined in Table A1-7 converted to linear scale.

If non-ULA arrays are used, the equations must be modified. For arbitrary array configurations on the horizontal plane, see Fig. 10, the distance term d_u in equations (23) and (20) is replaced by:

$$d'_{u,n,m} = \frac{\sqrt{x_u^2 + y_u^2} \cos(\arctan(y_u/x_u) - \varphi_{n,m})}{\sin \varphi_{n,m}}, \quad (24)$$

where (x_u, y_u) are the co-ordinates of the u th element A_u and A_0 is the reference element.

FIGURE 10

Modified distance of antenna element u with non-ULA array

Step 10b: Generate channel coefficients for each cluster n and each receiver and transmitter element pair u,s . Alternatively to Step 10a channel coefficients can be generated by applying the so called correlation matrix based method. Temporal correlations (Doppler effect) are introduced either by filtering independent and identically distributed complex Gaussian sequences with a proper Doppler spectrum shaping filter or by applying some equivalent method. MIMO antenna correlations are introduced by performing a linear transformation to the temporally correlated sequences. Unique covariance matrices are determined for each drop and radio link based on the parameters defined in the previous steps. The MIMO covariance matrix can be composed of transmitter and receiver spatial correlation matrices, and by the polarization covariance matrices with the Kronecker product of matrices. Spatial correlation matrices can be derived for each cluster directly from the ChIRs of Step 10a [Kermoal, *et al.*, 2002; Smith and Shafi, 2004]. Alternatively, spatial correlation matrices and the polarization covariance matrices can be derived from the antenna configuration and the model parameters (AoA, AoD) determined in Step 7 with XPR parameter from Table A1-7*.

Step 11: Apply path loss and shadowing for the channel coefficients. This is valid only for system level simulations.

* WiMAX Forum, WiMAX Forum Mobile Release 1.0 Channel Model, June 2008, available at http://www.wimaxforum.org/technology/documents/wimax_forum_mobile_release_1_0_channel_model_v100.pdf.

TABLE A1-7
Channel model parameters

In Table A1-7: DS: rms delay spread, ASD: rms azimuth spread of departure angles, ASA: rms azimuth spread of arrival angles, SF: shadow fading, and K : Ricean K -factor.

The sign of the shadow fading is defined so that positive SF means more received power at UT than predicted by the path loss model.

Scenarios		InH		UMi			SMa		UMa		RMa	
		LoS	NLoS	LoS	NLoS	O-to-I	LoS	NLoS	LoS	NLoS	LoS	NLoS
Delay spread (DS) log ₁₀ (s)	μ	-7.70	-7.41	-7.19	-6.89	-6.62	-7.23	-7.12	-7.03	-6.44	-7.49	-7.43
	σ	0.18	0.14	0.40	0.54	0.32	0.38	0.33	0.66	0.39	0.55	0.48
AoD spread (ASD) log ₁₀ (degrees)	μ	1.60	1.62	1.20	1.41	1.25	0.78	0.90	1.15	1.41	0.90	0.95
	σ	0.18	0.25	0.43	0.17	0.42	0.12	0.36	0.28	0.28	0.38	0.45
AoA spread (ASA) log ₁₀ (degrees)	μ	1.62	1.77	1.75	1.84	1.76	1.48	1.65	1.81	1.87	1.52	1.52
	σ	0.22	0.16	0.19	0.15	0.16	0.20	0.25	0.20	0.11	0.24	0.13
Shadow fading (SF) (dB)	σ	3	4	3	4	7	4	8	4	6	4	8
K -factor (K) (dB)	μ	7	N/A	9	N/A	N/A	9	N/A	9	N/A	7	N/A
	σ	4	N/A	5	N/A	N/A	7	N/A	3.5	N/A	4	N/A
Cross-correlations*	ASD vs DS	0.6	0.4	0.5	0	0.4	0	0	0.4	0.4	0	-0.4
	ASA vs DS	0.8	0	0.8	0.4	0.4	0.8	0.7	0.8	0.6	0	0
	ASA vs SF	-0.5	-0.4	-0.4	-0.4	0	-0.5	0	-0.5	0	0	0
	ASD vs SF	-0.4	0	-0.5	0	0.2	-0.5	-0.4	-0.5	-0.6	0	0.6
	DS vs SF	-0.8	-0.5	-0.4	-0.7	-0.5	-0.6	-0.4	-0.4	-0.4	-0.5	-0.5
	ASD vs ASA	0.4	0	0.4	0	0	0	0	0	0.4	0	0
	ASD vs K	0	N/A	-0.2	N/A	N/A	0	N/A	0	N/A	0	N/A
	ASA vs K	0	N/A	-0.3	N/A	N/A	0	N/A	-0.2	N/A	0	N/A
	DS vs K	-0.5	N/A	-0.7	N/A	N/A	0	N/A	-0.4	N/A	0	N/A
SF vs K	0.5	N/A	0.5	N/A	N/A	0	N/A	0	N/A	0	N/A	
Delay distribution		Exp	Exp	Exp	Exp	Exp	Exp	Exp	Exp	Exp	Exp	
AoD and AoA distribution		Laplacian		Wrapped Gaussian			Wrapped Gaussian		Wrapped Gaussian		Wrapped Gaussian	
Delay scaling parameter r_τ		3.6	3	3.2	3	2.2	2.4	1.5	2.5	2.3	3.8	1.7
XPR (dB)	μ	11	10	9	8.0	9	8	4	8	7	12	7
Number of clusters		15	19	12	19	12	15	14	12	20	11	10
Number of rays per cluster		20	20	20	20	20	20	20	20	20	20	20
Cluster ASD		5	5	3	10	5	5	2	5	2	2	2
Cluster ASA		8	11	17	22	8	5	10	11	15	3	3
Per cluster shadowing std ζ (dB)		6	3	3	3	4	3	3	3	3	3	3
Correlation distance (m)	DS	8	5	7	10	10	6	40	30	40	50	36
	ASD	7	3	8	10	11	15	30	18	50	25	30
	ASA	5	3	8	9	17	20	30	15	50	35	40
	SF	10	6	10	13	7	40	50	37	50	37	120
	K	4	N/A	15	N/A	N/A	10	N/A	12	N/A	40	N/A

1.3.2.2 Reduced variability models (Optional)

The CDL model is intended for calibration purposes only. Each cluster is composed of 20 rays with fixed offset angles and identical power. In the case of a cluster where a ray of dominant power exists, the cluster has 20 + 1 rays. This dominant ray has zero angle offset. The departure and arrival rays are coupled randomly. The CDL tables of all scenarios of interest are given below, where the cluster power and the power of each ray are tabulated. The CDL models offer well-defined radio channels with fixed parameters to obtain comparable simulation results with relatively

non-complicated channel models. Delay spread and azimuth spreads medians of the CDL models are equal to median values given in Table A1-8.

TABLE A1-8

Expectation (median) output values for large scale parameters

Scenario		DS (ns)	AS at BS (degrees)	AS at UT (degrees)
InH	LoS	20	40	42
	NLoS	39	42	59
UMi	LoS	65	16	56
	NLoS	129	26	69
	O-to-I	49	18	58
SMa	LoS	59	6	30
	NLoS	75	8	45
UMa	LoS	93	14	65
	NLoS	365	26	74
RMa	LoS	32	8	33
	NLoS	37	9	33

CDL models can be implemented as described either in Step 10a or in Step 10b.

InH – Indoor hotspot

The CDL parameters of LoS and NLoS condition are given below. In the LoS model the Ricean K factor is 5 dB.

TABLE A1-9

Scenario InH LoS clustered delay line model, indoor hotspot

Cluster No.	Delay (ns)	Power (dB)	AoD (degrees)	AoA (degrees)	Ray power (dB)		Cluster ASD = 5°	Cluster ASA = 8°	XPR = 11 dB
					-0.01 ⁽¹⁾	-41.7 ⁽²⁾			
1	0	0	0	0	-0.01 ⁽¹⁾	-41.7 ⁽²⁾			
2	10	-15.7	79	85		-28.7			
3	25	-10.5	-84	73		-23.5			
4	25	-16.7	-97	-82		-29.7			
5	30	-17.6	-102	-72		-30.6			
6	35	-14.1	80	-64		-27.2			
7	40	-12.9	69	-73		-25.9			
8	50	-19.5	104	-83		-32.5			
9	55	-21.8	98	96		-34.8			
10	60	-20.8	98	-91		-33.8			
11	65	-24.1	-113	-93		-37.1			
12	85	-13.9	-79	74		-26.9			
13	90	-20.1	-109	-87		-33.1			
14	100	-18	89	-77		-31			
15	130	-21	95	-97		-34			

⁽¹⁾ Power of dominant ray.

⁽²⁾ Power of each other ray.

TABLE A1-10

Scenario InH NLoS clustered delay line model, indoor hotspot

Cluster No.	Delay (ns)	Power (dB)	AoD (degrees)	AoA (degrees)	Ray power (dB)
1	0	-2.4	-34	50	-15.4
2	15	-1.9	34	50	-15
3	20	-8.1	60	-83	-21.1
4	25	-1.8	24	-30	-14.8
5	30	0	-1	-3	-13
6	40	-2.3	-31	44	-15.4
7	55	-3.7	55	-63	-16.8
8	60	-8.4	69	-105	-21.4
9	60	-3.2	34	-61	-16.2
10	70	-9.7	-73	110	-22.7
11	75	-6.2	-55	-85	-19.2
12	75	-8.9	56	-85	-21.9
13	90	-4	-47	58	-17
14	150	-14.1	-84	121	-27.1
15	160	-12.1	87	-109	-25.1
16	170	-10.6	71	108	-23.6
17	195	-19.6	-99	139	-32.6
18	205	-16.8	-99	-137	-29.8
19	225	-13.5	86	124	-26.5

Cluster ASD = 5°
Cluster ASA = 11°
XPR = 10 dB

UMi – Urban micro-cell

In the LoS model the Ricean K -factor is 6 dB.

TABLE A1-11

Scenario UMi: LoS clustered delay line model, urban micro-cell

Cluster No.	Delay (ns)			Power (dB)			AoD (degrees)	AoA (degrees)	Ray power (dB)	
1	0			0			0	0	-0.20 ⁽¹⁾	-28.8 ⁽²⁾
2	30	35	40	-15.6	-17.8	-19.6	31	-108	-25.6	
3	85			-14.0			35	153	-27.0	
4	135	140	145	-15.8	-18.0	-19.8	-38	-111	-25.8	
5	160			-20.7			45	179	-33.7	
6	195			-17.3			-46	-150	-30.3	
7	210			-21.8			46	-163	-34.8	
8	255			-17.7			-43	166	-30.7	
9	280			-21.6			-47	14	-34.6	
10	340			-23.0			51	-4	-36.0	
11	360			-24.5			-62	43	-37.5	
12	420			-25.0			-58	44	-38.0	

Cluster ASD = 3°
Cluster ASA = 17°
XPR = 9 dB

⁽¹⁾ Power of dominant ray.

⁽²⁾ Power of each other ray.

TABLE A1-12

Scenario UMi: NLoS clustered delay line model, urban micro-cell

Cluster No.	Delay (ns)			Power (dB)			AoD (degrees)	AoA (degrees)	Ray power (dB)
1	0			-6.7			31	-83	-19.8
2	10	15	10	-4.9	-7.1	-8.9	10	54	-14.7
3	20			-1.9			26	37	-14.9
4	35			-6.3			-27	96	-19.3
5	40	45	50	-3	-5.2	-7	-3	3	-13.0
6	55			-7.5			29	-86	-20.5
7	55			-6.4			-33	84	-19.4
8	200			-10.8			37	-112	-23.9
9	205			-5.2			-29	-78	-18.2
10	250			-4.9			27	65	-17.9
11	330			-9.2			-35	-88	-22.3
12	440			-15.5			-48	-130	-28.5
13	440			-16.7			-50	153	-29.7
14	515			-12.4			-44	106	-25.5
15	530			-16.9			46	147	-29.9
16	580			-12.7			-45	118	-25.7
17	590			-23.5			-59	-178	-36.5
18	625			-22.1			60	-163	-35.1
19	730			-23.6			56	163	-36.6

Cluster ASD = 10°
Cluster ASA = 22°
XPR = 8 dB

TABLE A1-13

Scenario UMi: Outdoor-to-indoor clustered delay line model, urban micro-cell

Cluster No.	Delay (ns)			Power (dB)			AoD (degrees)	AoA (degrees)	Ray power (dB)
1	0	5	10	-3.0	-5.2	-7.0	0	0	-13.0
2	0			-8.7			32	102	-21.7
3	5			-3.7			-21	-66	-16.7
4	10			-11.9			37	-119	-24.9
5	35			-16.2			-43	139	-29.2
6	35			-6.9			28	91	-19.9
7	65	70	75	-3.4	-5.6	-7.3	-49	157	-13.4
8	120			-10.3			-34	-111	-23.3
9	125			-20.7			-49	157	-33.7
10	195			-16.0			43	138	-29.1
11	250			-21.0			49	158	-34.0
12	305			-22.9			51	165	-35.9

Cluster ASD = 3°
Cluster ASA = 8°
XPR = 9 dB

UMa – Urban macro-cell

In the LoS model the Rician K -factor is 5.0 dB.

TABLE A1-14

Scenario UMA: LoS clustered delay line model, urban macro-cell

Cluster No.	Delay (ns)			Power (dB)			AoD (degrees)	AoA (degrees)	Ray power (dB)	
1	0			0			0	0	-0.23 ⁽¹⁾	-26.5 ⁽²⁾
2	15	20	25	-15.4	-17.6	-19.4	36	143	-25.4	
3	30			-12.6			-28	-156	-25.6	
4	45	50	55	-14.1	-16.3	-18.1	-25	133	-24.1	
5	220			-19.4			42	180	-32.4	
6	310			-23.8			-40	19	-36.8	
7	365			-16.7			-28	161	-29.7	
8	440			-19.4			-35	3	-32.4	
9	450			-24.8			-47	40	-37.8	
10	535			-21.3			-39	-37	-34.3	
11	595			-23.9			47	-36	-36.9	
12	640			-25.0			-43	-48	-38.0	

Cluster ASD = 5°

Cluster ASA = 11°

XPR = 8 dB

⁽¹⁾ Power of dominant ray.⁽²⁾ Power of each other ray.

TABLE A1-15

Scenario UMA: NLoS clustered delay line model, urban macro-cell

Cluster No.	Delay (ns)			Power (dB)			AoD (degrees)	AoA (degrees)	Ray power (dB)	
1	0	5	10	-3.5	-5.7	-7.5	6	29	-13.5	
2	5			-9.2			44	-98	-22.2	
3	20	25	30	-3.0	-5.2	-7.0	2	8	-13.0	
4	45			-7.8			-34	-114	-20.8	
5	265			-3.7			26	70	-16.7	
6	290			-8.6			-41	107	-21.6	
7	325			-2.5			-17	59	-15.5	
8	340			-7.3			-33	-103	-20.3	
9	355			-3.8			24	73	-16.8	
10	440			-6.9			-34	-111	-19.9	
11	555			-8.9			-38	-112	-21.9	
12	645			-9.0			44	122	-22.0	
13	970			-9.8			53	129	-22.8	
14	1 015			-15.0			54	153	-28.0	
15	1 220			-13.4			53	-145	-26.4	
16	1 395			-14.9			52	-157	-27.9	
17	1 540			-16.7			57	-178	-29.7	
18	1 750			-11.2			53	-114	-24.2	
19	1 870			-18.2			-54	-160	-31.2	
20	1 885			-17.8			-60	-175	-30.8	

Cluster ASD = 2°

Cluster ASA = 15°

XPR = 7 dB

SMA – Sub-urban macro-cell (Optional)In the LoS model the Rician K -factor is 4 dB.

TABLE A1-16

Scenario SMA: LoS clustered delay line model, suburban

Cluster No.	Delay (ns)			Power (dB)			AoD (degrees)	AoA (degrees)	Ray power (dB)	
1	0	5	10	0.0	-25.3	-27.1	0	0	-0.02 ⁽¹⁾	-33.1 ⁽²⁾
2	85			-21.6			-29	-144	-34.7	
3	135			-26.3			-32	-159	-39.3	
4	135			-25.1			-31	155	-38.1	
5	170			-25.4			31	156	-38.4	
6	190			-22.0			29	-146	-35.0	
7	275			-29.2			-33	168	-42.2	
8	290	295	300	-24.3	-26.5	-28.2	35	-176	-34.3	
9	290			-23.2			-30	149	-36.2	
10	410			-32.2			35	-176	-45.2	
11	445			-26.5			-32	-159	-39.5	
12	500			-32.1			35	-176	-45.1	
13	620			-28.5			33	-165	-41.5	
14	655			-30.5			34	-171	-43.5	
15	960			-32.6			35	177	-45.6	

Cluster ASD = 5°, Cluster ASA = 5°

XPR = 8 dB

⁽¹⁾ Power of dominant ray.⁽²⁾ Power of each other ray.

TABLE A1-17

Scenario SMA: NLoS clustered delay-line model, suburban

Cluster No.	Delay (ns)			Power (dB)			AoD (degrees)	AoA (degrees)	Ray power (dB)
1	0	5	10	-3.0	-5.2	-7.0	0	0	-13.0
2	25			-7.5			13	-71	-20.5
3	35			-10.5			-15	-84	-23.5
4	35			-3.2			-8	46	-16.2
5	45	50	55	-6.1	-8.3	-10.1	12	-66	-16.1
6	65			-14.0			-17	-97	-27.0
7	65			-6.4			12	-66	-19.4
8	75			-3.1			-8	-46	-16.1
9	145			-4.6			-10	-56	-17.6
10	160			-8.0			-13	73	-21.0
11	195			-7.2			12	70	-20.2
12	200			-3.1			8	-46	-16.1
13	205			-9.5			14	-80	-22.5
14	770			-22.4			22	123	-35.4

Cluster ASD = 2°, Cluster ASA = 10°

XPR = 4 dB

RMa – Rural macro-cell

The CDL parameters for LoS and NLoS conditions are given below. In the LoS model the Ricean *K*-factor is 6 dB.

TABLE A1-18

Scenario RMa: LoS Clustered delay line model, rural

Cluster No.	Delay (ns)			Power (dB)			AoD (degrees)	AoA (degrees)	Ray power (dB)	
1	0	5	10	0.0	-17.8	-19.5	0	0	-0.12 ⁽¹⁾	-25.6 ⁽²⁾
2	35	40	45	-16.9	-19.1	-20.9	24	99	-26.9	
3	45			-16.8			23	95	-29.8	
4	65			-18.3			24	99	-31.3	
5	65			-21.2			-25	-106	-34.2	
6	110			-17.1			-23	96	-30.1	
7	125			-19.7			-25	-103	-32.7	
8	125			-23.8			27	113	-36.8	
9	170			-22.9			27	110	-35.9	
10	170			-20.9			25	106	-33.9	
11	200			-21.9			-26	-108	-34.9	

Cluster ASD = 2°

Cluster ASA = 3°

XPR = 12 dB

⁽¹⁾ Power of dominant ray.⁽²⁾ Power of each other ray.

TABLE A1-19

Scenario RMa: NLoS clustered delay line model, rural

Cluster No.	Delay (ns)			Power (dB)			AoD (degrees)	AoA (degrees)	Ray power (dB)	
1	0			-4.9			-12	-46	-17.9	
2	0			-7.8			16	58	-20.8	
3	5	10	15	-3.0	-5.2	-7.0	0	0	-13.0	
4	5			-2.7			9	34	-15.7	
5	10			-2.6			-9	34	-15.6	
6	15	20	25	-3.6	-5.8	-7.5	13	49	-13.6	
7	15			-2.7			-9	-34	-15.7	
8	55			-5.6			13	49	-18.6	
9	110			-7.3			15	56	-20.3	
10	220			-10.3			18	67	-23.3	

Cluster ASD = 2°

Cluster ASA = 3°

XPR = 7 dB

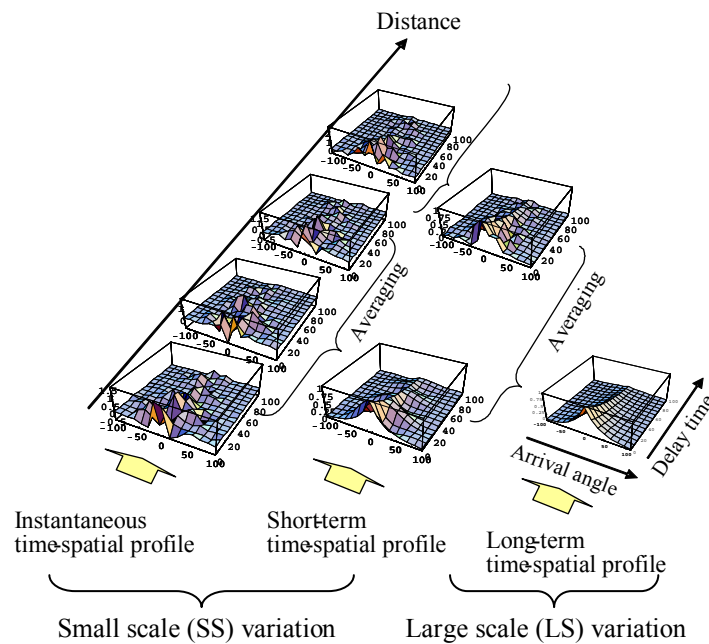
1.4 Extension module

The purpose of the extension module is to generate parameters for Table A1-7 relating to the primary model and Tables A1-14 to A1-19 relating to the CDL model for macro-cell scenarios such as UMa, SMa and RMa as described in the primary module in § 1.3. The extension module provides additional level of parameter variability. In the primary module, SS and LS parameters are variables, and the extension module provides new parameter values for the primary module based on environment-specific parameters. The channel impulse responses are generated in the primary module according to Steps 1 to 11 described in § 1.3.2.1.

The extension module is based on the time-spatial propagation model (TSP model) described in Recommendation ITU-R P.1816 [Fujii, 2004 ; Ohta and Fujii, 2006 and Omote and Fujii, 2007]. The TSP model is a geometry-based double directional channel model with closed-form functions. It calculates the large scale parameters for the channel realization by taking into account the following key parameters such as city structures (street width, average building height), BS height, bandwidth and the distance between the BS and the UT. The channel models are targeted for up to 100 MHz RF bandwidth.

The TSP model consists of three profile models, which are long-term time-spatial profile model, Short-term time-spatial profile model, and Instantaneous time-spatial profile model, see Fig. 11. The time-spatial profile is the joint delay-AoA power spectrum. This will vary with the distance. The snapshot of the time-spatial profile at a given distance is called instantaneous time-spatial profile. The average of the time-spatial profile over several tens of wavelengths is the short-term time-spatial profile. The average of the time-spatial profile over hundreds of wavelengths is the long-term time-spatial profile. The delay profiles arrival angular profiles are generated by the time-spatial profile model, as shown in Fig. 12.

FIGURE 11
Time-spatial propagation (TSP) model for base coverage macrocell



Large scale parameters (e.g., delay spread and angle spread) in the primary module are calculated from the Long-term time-spatial profile model. Reduced variability models in the extension module are calculated from both long-term and short-term time-spatial profile models, which are detailed in § 1.4.2.

FIGURE 12
Delay and angular profiles for base coverage macrocell

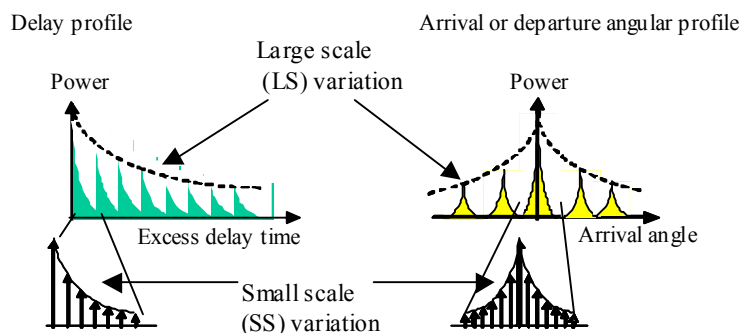


Figure 13 shows the concept of using the TSP model to generate a time-spatial profile. After providing to the model the key parameters like carrier frequency, bandwidth, city structure such as average building height, road width, BS antenna height, and distance from the BS, a time-spatial profile is generated by setting the pseudo-random number generator.

FIGURE 13
Generation of TSP model

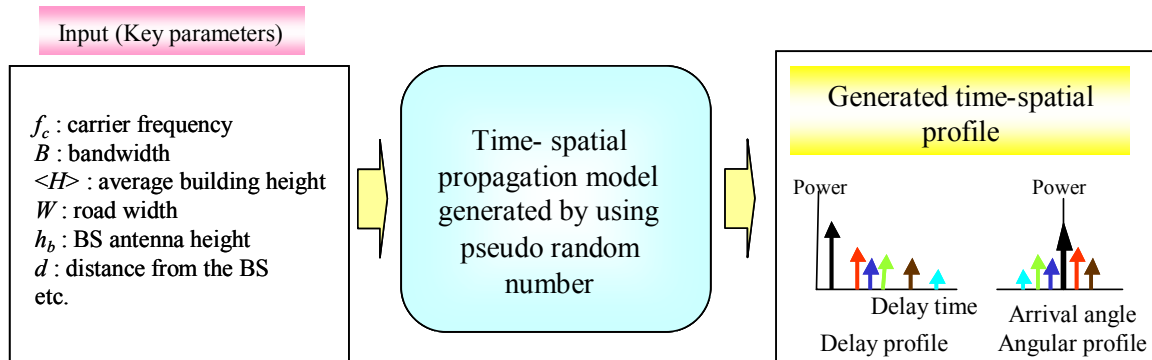


Table A1-20 shows key parameters of the TSP model and their applicable ranges.

Table A1-21 shows the parameter values of the city structures for the UMa, SMa and RMa scenarios. By using Table A1-21, a time-spatial channel model that can evaluate simulation conditions different from those described in Table 8-1.

TABLE A1-20

Key parameters in TSP model

Condition	Key parameter	Symbol	Applicable range
Frequency conditions	Carrier frequency (MHz)	f_c	400-6 000 MHz
	Bandwidth or chip rate (MHz)	B	0.5-100 MHz
City structures	Average building height (m)	$\langle H \rangle$	5-50 m: (height above the UT ground level)
	Road width (m)	W	5-50 m
Cell conditions	BS antenna height (m)	h_b	10-150 m (height above the UT ground level)
	UT antenna height (m)	h_m	1-10 m
	Distance from the BS (m)	d	50-5 000 m

TABLE A1-21

Parameter values for city structures

Key parameters		Average building height, $\langle H \rangle$ (m)	Road width, W (m)
City structure			
(*)	Dense urban	30	20
UMa	Urban	20	20
SMa	Suburban	10	20
(*)	Residential	8	20
RMa	Rural	5	20

1.4.1 Large scale parameters

1.4.1.1 NLoS scenarios

Formulas for empirical path-loss, power delay profile, departure angular profile, and arrival angular profile for Base coverage macro-cellular scenarios such as SMA, UMa and RMa, which can take the city structure into account and suit carrier frequencies up to the SHF band, are given below:

a) Path-loss model

An empirical propagation loss formula, which can take the city structure into account and suits carrier frequencies up to the SHF band, is given as follows [Fujii, 2003]:

$$Loss_L(d) = 101.04 - 7.1 \log W + 7.5 \log \langle H \rangle - \{24.37 - 3.7(\langle H \rangle / h_b)^2\} \log h_b + (43.42 - 3.1 \log h_b) \log(d/1000) + 20 \log f_c - a(h_m) \quad \text{dB} \quad (25)$$

where d denotes the distance between the BS and the UT. h_b (m), $\langle H \rangle$ (m), and W denote the BS antenna height (m), the average building height, and the street width, respectively. f_c denotes the carrier frequency (MHz). $a(h_m)$ is a correction factor for mobile antenna height h_m (m) defined as follows:

$$a(h_m) = 3.2(\log(11.75h_m))^2 - 4.97 \quad \text{dB} \quad (26)$$

b) Power delay profile model

An empirical long-term path delay profile model $PDP_L(i, d)$ that takes into account the city structure and that suits carrier frequencies up to the SHF band and bandwidth B (MHz) up to 100 MHz is recommended as Recommendation ITU-R P.1816. The delay profile normalized by the first cluster's power is given as follows [Fujii, 2004 and Ohta and Fujii, 2006]:

$$PDP_L(i, d) = \alpha(d) \log(1+i) + 10 \log c(i) \quad (27)$$

where:

$$\alpha(d) = -\{19.1 + 9.68 \log(h_b / \langle H \rangle)\} B^{\{-0.36 + 0.12 \log(h_b / \langle H \rangle)\}} (d/1000)^{\{-0.38 + 0.21 \log(B)\}} \quad (28)$$

$$c(i) = \begin{cases} 1 & (i=0) \\ \min\left(0.63, \left\{0.59e^{-0.017B} + (0.017 + 0.0004B)\langle H \rangle\right\} e^{-\{(0.077 - 0.00096B) - (0.0014 - 0.000018B)\langle H \rangle\}i}\right) & (i \geq 1) \end{cases} \quad (29a)$$

(0.5 ≤ B ≤ 50 Mcps)

$$c(i) = \begin{cases} 1 & (i=0) \\ \min\left(0.63, \left\{0.59e^{-0.0172B} + (0.0172 + 0.0004B) \langle H \rangle\right\} e^{-\left[0.0878e^{-0.0218B} - (0.0014 - 0.000018B) \langle H \rangle\right]i}\right) & (i \geq 1) \end{cases} \quad (29b)$$

(0.5 < B ≤ 100 Mcps)

Here i represents the path number ($i = 0, 1, 2, \dots$) in the sense of an excess delay time normalized by the time resolution $1/B$.

The power delay profile normalized by the total power of all clusters is given by:

$$PDP_{LN}(i, d) = PDP_L(i, d) - PDP_{norm}(d) \quad \text{dB} \quad (30)$$

where $PDP_{norm}(d)$ represents the total power of all clusters:

$$PDP_{norm}(d) = 10 \log \left(\sum_{i=0} 10^{PDP_L(i, d)/10} \right) \quad \text{dB} \quad (31)$$

The path number i can be changed to the excess delay time τ (μs) by using the following relation:

$$\tau = i / B \Rightarrow i = \tau B \quad (32)$$

The delay profile $PDP_L(\tau, d)$ can be calculated as:

$$PDP_L(\tau, d) = \alpha(d) \log(1 + \tau B) + 10 \log c(\tau B) \quad \text{dB} \quad (33)$$

c) Departure angular profile model

An empirical long-term arrival angular profile model $AOD_L(\theta, d)$, which can take the city structure into account and that suits carrier frequencies up to the SHF band and bandwidth B (MHz) up to 100 MHz, is recommended as Recommendation ITU-R P.1816. The departure angular profile around the BS normalized by the first cluster's power is given as follows (see Recommendation ITU-R P.1816 and [Omote and Fujii, 2007]):

$$AOD_L(\theta, d) = 10 \log(1 + |\theta|/a)^{-\beta} \quad (|\theta| \leq \theta_{max}) \quad \text{dB} \quad (34)$$

where:

$$a = -\frac{0.2d}{1000} + 2.1 \left\{ \left(\frac{\langle H \rangle}{h_b} \right)^{0.23} \right\} \quad (35)$$

$$\beta = (-0.015 \langle H \rangle + 0.63) d / 1000 - 0.16 + 0.76 \log(h_b)$$

d) Arrival angular profile model

The arrival angular profile around the MT of each cluster is given by:

$$AOA_L(\theta, d) = \exp[-|\theta|/\theta_{AOA}] \quad (|\theta| \leq 180^\circ) \quad (36)$$

where θ_{AOA} denotes the angle spread of AOA. $AOA_L(\theta, d)$ does not depend on the distance, d .

1.4.1.2 LoS scenarios

Formulas for empirical path-loss, power delay profile, departure angular profile, and arrival angular profile for LoS Base coverage macro-cellular scenarios such as SMA and UMA, which can take the city structure into account and suit carrier frequencies up to the SHF band, are given in the following.

a) Path-loss model

The loss formula consists of formulas that cover the cases before and after the break point, B_p , which is defined by:

$$B_p = \frac{2\pi h_b h_m}{\lambda} \quad (37)$$

λ (m) denotes the wavelength and is given by $300/f_c$. An empirical propagation loss formula before the break point B_p is given as follows:

$$\begin{aligned} Loss_{LLOS}(d) = & 20 \log(4\pi d / \lambda) + (\min(0.03 < H >^{1.72}, 10)) \log(d) \\ & - \min(0.044 < H >^{1.72}, 14.77) + (0.002 \log < H >) d \quad (d \leq B_p) \end{aligned} \quad (38)$$

An empirical propagation loss formula after the break point B_p , is expressed as follows:

$$\begin{aligned} Loss_{LLOS}(d) = & 40 \log(1000d) - 20 \log h_b - 20 \log h_m + 5 \log f_c \\ & + 11 \log < H > - 7.1 \log W - 2.45 \quad (B_p \leq d) \end{aligned} \quad (39)$$

b) Power delay profile model

An empirical long-term delay profile model $PDP_{LLOS}(l, d)$ normalized by the first cluster's power is given by:

$$PDP_{LLOS}(l, d) = PDP_{L, direct}(l, d) + 10^{PDP_{L, scatter}(l, d)/10} \quad (40)$$

where:

$$PDP_{L, direct}(l, d) = \delta(l) + 0.3\delta(l - W^2/d) + 0.1\delta(l - 3W^2/d) \quad (41)$$

$$PDP_{L, scatter}(l, d) = PDP_L(l, d) - 12 \quad \text{dB} \quad (42)$$

$\delta(l)$ represents a delta function defined as $\delta(l) = 1$ for $l = 1$ and $\delta(l) = 0$ for $l \neq 0$. $PDP_L(l, d)$ is given by the NLOS power delay profile model.

The K -factor of the first cluster ($l = 0$) is given from equations (41) and (42) as follows:

$$K = 12 \quad \text{dB} \quad (43)$$

c) Departure angular profile model

An empirical long-term departure angular profile model $AOD_{LLOS}(\theta, d)$ with departure angle θ normalized by the first cluster's power is given as follows:

$$AOD_{LLOS}(\theta, d) = AOD_{L, direct}(\theta, d) + 10^{AOD_{L, scatter}(\theta, d)/10} \quad (44)$$

where:

$$AOD_{L,direct}(\theta, d) = \delta(\theta) + 0.3\delta(\theta - W/d \cdot (180/\pi)) + 0.1\delta(\theta - 2W/d \cdot (180/\pi)) \quad (45)$$

$$AOD_{L,scatter}(\theta, d) = AOD_L(\theta, d) - 12 \quad \text{dB} \quad (46)$$

Here, $AOD_L(\theta, d)$ is given by the NLoS departure angular profile model.

d) Arrival angular profile model

An empirical long-term arrival angular profile model $AOD_{LLOS}(\theta, d)$ with arrival angle θ normalized by the first cluster's power is given as follows:

$$AOA_{LLOS}(\theta, d) = AOA_{L,direct}(\theta, d) + 10^{AOA_{L,scatter}(\theta, d)/10} \quad (47)$$

where:

$$AOA_{L,direct}(\theta, d) = \delta(\theta) + 0.3\delta(\theta - 2W/d \cdot (180/\pi)) + 0.1\delta(\theta + 2W/d \cdot (180/\pi)) \quad (48)$$

$$AOA_{L,scatter}(\theta, d) = AOA_L(\theta, d) - 12 \quad \text{dB} \quad (49)$$

Here, $AOA_L(\theta, d)$ is given by the NLoS arrival angular profile model.

1.4.1.3 XPD

XPD represents cross-polarization discrimination; its value (dB) is given by:

$$XPD_L = 15 - 10(1.5h_b / \langle H \rangle + 1)^{-0.35} \quad \text{dB} \quad (50)$$

XPD_L depends on the city structures.

1.4.1.4 Building penetration loss

An empirical building penetration loss formula $Loss_{Pene}(d_p, h_f)$ is expressed as follows [Okamoto and Ichitsubo, 2005]:

$$Loss_{Pene}(d_p, h_f) = 0.6d_p - 0.6h_f + 10 \quad \text{(dB)} \quad (51)$$

where h_f (m) denotes the height of the floor where the UT is located and d_p (m) denotes the entry distance from the nearest window to the UT on the floor where the UT is located. The floor height can be changed to the floor number $N_F (= 1, 2, \dots)$ by using the height per floor Δh_f as follows:

$$Loss_{Pene}(d_p, h_f) = 0.6d_p - 0.6(N_F - 1)\Delta h_f + 10 \quad \text{(dB)} \quad (N_F = 1, 2, \dots) \quad (52)$$

Therefore, the propagation loss $Loss_L^{O \rightarrow I}(d)$ from outdoor BS to indoor UT can be expressed by adding the building penetration loss $Loss_{Pene}(d_p, h_f)$ to the propagation loss $Loss_L(d)$ on the street next to the building as follows:

$$Loss_L^{O \rightarrow I}(d) = Loss_L(d) + Loss_{Pene}(d_p, h_f) \quad \text{(dB)} \quad (53)$$

1.4.1.5 Short-term variation

The short-term variation is generally caused by shadow effects. It can be assumed it follows a log-normal distribution with its power spectrum being:

$$P_s(f) = \begin{cases} \frac{\sigma_s^2}{2f_s} & (|f| \leq f_s) \\ 0 & (|f| > f_s) \end{cases} \quad (54)$$

where σ_s^2 is the average power of the short-term variation and is usually given by the normalized power of 1. Typical standard deviation of log-normal shadowing is set to 4.5 dB for macro-cell environments. f_s , the maximum frequency of the short-term variation, and depends on the environment and bandwidth as follows:

$$f_s = v/(110B^{-0.146} <H>^{0.058}) \quad (55)$$

where v (m) is the speed of the UT.

1.4.1.6 Spreads and their variations of PDP, AoD and AoA in large scale parameters

a) The spread of PDP

The delay spread $\sigma_{PDP}(d)$ at distance d from the BS is expressed as:

$$\sigma_{PDP}(d) = \sqrt{\frac{\int_0^{\tau_{\max}(d)} (\tau - T_{PDP}(d))^2 10^{PDP_L(\tau,d)/10} d\tau}{\int_0^{\tau_{\max}(d)} 10^{PDP_L(\tau,d)/10} d\tau}} \quad (56)$$

where $T_{PDP}(d)$ is the average delay time at distance d from BS given by:

$$T_{PDP}(d) = \frac{\int_0^{\tau_{\max}(d)} \tau 10^{PDP_L(\tau,d)/10} d\tau}{\int_0^{\tau_{\max}(d)} 10^{PDP_L(\tau,d)/10} d\tau} \quad (57)$$

$\tau_{\max}(d)$ (μ s) is the maximum delay time determined from the threshold level ΔL_{th} (dB) (>0); it must satisfy the following equation:

$$PDP_L(\tau_{\max}(d), d) = -\Delta L_{th} \quad (58)$$

Assuming that the UT is located uniformly in the cell area, the average delay spread μ_{PDP} and its standard deviation $\sigma_{\sigma_{PDP}}$ over the whole cell area covered with cell radii of d_{\min} and d_{\max} are given respectively by

$$\mu_{PDP} = \int_{d_{\min}}^{d_{\max}} \sigma_{PDP}(r) \frac{2\pi r}{\pi(d_{\max}^2 - d_{\min}^2)} dr \quad (59)$$

$$\sigma_{\sigma_{PDP}} = \sqrt{\int_{d_{\min}}^{d_{\max}} (\sigma_{PDP}(r) - \mu_{PDP})^2 \frac{2\pi r}{\pi(d_{\max}^2 - d_{\min}^2)} dr} \quad (60)$$

b) The spread of AoD

The angular spread $\sigma_{AOD}(d)$ at distance d from BS is expressed by:

$$\sigma_{AOD}(d) = \sqrt{\frac{\int_{-\theta_{\max}(d)}^{\theta_{\max}(d)} (\theta - T_{AOD}(d))^2 \cdot 10^{AOD_L(\theta,d)/10} d\theta}{\int_{-\theta_{\max}(d)}^{\theta_{\max}(d)} 10^{AOD_L(\theta,d)/10} d\theta}} \quad \text{degrees} \quad (61)$$

where $T_{AOD}(d)$ is the average AoD at distance d from the BS given by:

$$T_{AOD}(d) = \frac{\int_{-\theta_{\max}(d)}^{\theta_{\max}(d)} \theta \cdot 10^{AOD_L(\theta,d)/10} d\theta}{\int_{-\theta_{\max}(d)}^{\theta_{\max}(d)} 10^{AOD_L(\theta,d)/10} d\theta} \equiv 0 \quad \text{degrees} \quad (62)$$

$\theta_{\max}(d)$ (degrees) is the maximum AoD determined from the threshold level ΔL_{th} (dB) (>0); it must satisfy the following equation:

$$AOD_L(\theta_{\max}(d), d) = -\Delta L_{th} \quad \text{and} \quad \min(60, \theta_{\max}(d)) \Rightarrow \theta_{\max}(d) \quad (63)$$

In the case of NLoS, $\theta_{\max}(d)$ can be easily obtained by equation (64):

$$\theta_{\max}(d) = \min[60, a(d)(10^{\Delta L_{th}/10\beta(d)} - 1)] \quad (\text{deg.}) \quad (64)$$

Assuming that the UT is located uniformly in the cell area, the average delay spread μ_{AOD} and its standard deviation $\sigma_{\sigma_{AOD}}$ over the whole cell area covered with cell radii of d_{\min} and d_{\max} are given respectively by:

$$\mu_{AOD} = \int_{d_{\min}}^{d_{\max}} \sigma_{AOD}(r) \frac{2\pi r}{\pi(d_{\max}^2 - d_{\min}^2)} dr \quad \text{degrees} \quad (65)$$

$$\sigma_{\sigma_{AOD}} = \sqrt{\int_{d_{\min}}^{d_{\max}} (\sigma_{AOD}(r) - \mu_{AOD})^2 \frac{2\pi r}{\pi(d_{\max}^2 - d_{\min}^2)} dr} \quad \text{degrees} \quad (66)$$

c) The spread of AoA

The angular spread $\sigma_{AOA}(d)$ at distance d from the BS is expressed as:

$$\sigma_{AOA}(d) = \sqrt{\frac{\int_{-\theta_{\max}(d)}^{\theta_{\max}(d)} (\theta - T_{AOA}(d))^2 \cdot 10^{AOA_L(\theta,d)/10} d\theta}{\int_{-\theta_{\max}(d)}^{\theta_{\max}(d)} 10^{AOA_L(\theta,d)/10} d\theta}} \quad \text{degrees} \quad (67)$$

where $T_{AOA}(d)$ is the average AOA at distance d from the BS given by:

$$T_{AOA}(d) = \frac{\int_{-\theta_{\max}(d)}^{\theta_{\max}(d)} \theta \cdot 10^{AOA_L(\theta,d)/10} d\theta}{\int_{-\theta_{\max}(d)}^{\theta_{\max}(d)} 10^{AOA_L(\theta,d)/10} d\theta} \quad \text{degrees} \quad (68)$$

$\theta_{max}(d)$ (degrees) is the maximum AoA determined from the threshold level ΔL_{th} (dB) (>0); it must satisfy equation (69):

$$AOA_L(\theta_{max}(d), d) = -\Delta L_{th} \quad (69)$$

In the case of NLoS, $\theta_{max}(d)$ can be easily obtained by the equation (70):

$$\theta_{max}(d) = \min[180, \phi_{AI} \ln(10^{\Delta L_{th}/10})] = \min[180, 0.23\phi_{AI}\Delta L_{th}] \text{ (deg.)} \quad (70)$$

Assuming that the UT is located uniformly in the cell area, the average delay spread μ_{AOA} and its standard deviation $\sigma_{\sigma_{AOA}}$ over the whole cell area covered with cell radii of d_{min} and d_{max} are given respectively by:

$$\mu_{AOA} = \int_{d_{min}}^{d_{max}} \sigma_{AOA}(r) \frac{2\pi r}{\pi(d_{max}^2 - d_{min}^2)} dr \quad \text{degrees} \quad (71)$$

$$\sigma_{\sigma_{AOA}} = \sqrt{\int_{d_{min}}^{d_{max}} (\sigma_{AOA}(r) - \mu_{AOA})^2 \frac{2\pi r}{\pi(d_{max}^2 - d_{min}^2)} dr} \quad \text{degrees} \quad (72)$$

1.4.1.7 Large scale parameters in Table A1-7

Once the values for city structures in Table A1-15 and the threshold parameter in Table A1-22 have been set, the extension module can calculate the values of the parameters in Table A1-7.

TABLE A1-22

Threshold parameter

Parameter (dB)	Value (dB)
Threshold ΔL_{th}	25

The parameters calculated by the extension module correspond to those in Table A1-7 as follows:

For delay spread (DS), $\mu_{PDP} \rightarrow \mu$ and $\sigma_{\sigma_{PDP}} \rightarrow \sigma$

These parameters can be calculated by the following steps: equations (27) \rightarrow (56) \rightarrow (59) and (60) for NLoS, and equations (40) \rightarrow (56) \rightarrow (59) and (60) for LoS, respectively.

For AoD spread (ASD), $\mu_{AOD} \rightarrow \mu$ and $\sigma_{\sigma_{AOD}} \rightarrow \sigma$

These parameters can be calculated by the following steps: equations (34) \rightarrow (61) \rightarrow (65) and (66) for NLoS, and equations (44) \rightarrow (61) \rightarrow (65) and (66) for LoS, respectively.

For AoA spread (ASA), $\mu_{AOA} \rightarrow \mu$ and $\sigma_{\sigma_{AOA}} \rightarrow \sigma$

These parameters can be calculated by the following steps: equations (36) \rightarrow (67) \rightarrow (71) and (72) for NLoS, and equations (47) \rightarrow (67) \rightarrow (71) and (72) for LoS, respectively.

For XPR, $XPD_L \rightarrow \mu$

These parameters can be calculated by equation (50) for NLoS and LoS.

For shadow fading (SF), 4.5 dB $\rightarrow \sigma$

This parameter is a constant for NLoS and LoS.

For number of clusters, a constant number is generated (either 10 or 20).

The other parameters in Table A1-7 remain unchanged.

1.4.1.8 Time-spatial profile in cluster

a) Delay profile in the i th cluster

An empirical delay profile model $PDP_I(l_{ik})$ normalized by the first arrival path's power in the i th cluster is given as follows:

$$PDP_I(l_{ik}) = e^{-l_{ik}/l_I} \quad (0 \leq l_{ik} \leq l_{I\max}) \quad (73)$$

where l_I and $l_{I\max}$ denote the average excess path distance and the maximum excess path distance in the cluster, respectively. On the other hand, the excess path distance l (m) can be changed to the access delay time τ (μ s) by using the relation of $l = 300\tau$. The delay profile model in the cluster, $PDP_I(\tau_{ik})$, can then be determined by can then be determined by:

$$PDP_I(\tau_{ik}) = e^{-\tau_{ik}/\tau_I} \quad (0 \leq \tau_{ik} \leq \tau_{I\max}) \quad (74)$$

where τ_I and $\tau_{I\max}$ denote the excess average delay time and the maximum excess delay time in the cluster, respectively.

b) Departure angular profile in the i th cluster

An empirical departure angular profile model $AOD_I(\phi_{ik})$ with departure angle ϕ_{ik} in the i th cluster normalized by its central angular path's power is given as:

$$AOD_I(\phi_{ik}) = e^{-|\phi_{ik}|/\phi_{DI}} \quad (0 \leq |\phi_{ik}| \leq \phi_{DI\max}) \quad (75)$$

where:

$$\phi_{DI} = \frac{2l_{I\max}}{(d + 300\tau)} \cdot \left(\frac{180}{\pi}\right) = \frac{2(300\tau_{I\max})}{(d + 300\tau)} \cdot \left(\frac{180}{\pi}\right) \quad \text{degrees} \quad (76)$$

ϕ_{DI} depends on the excess delay time τ .

c) Arrival angular profile in the i th cluster

An empirical arrival angular profile model $AOA_I(\phi_{ik})$ with arrival angle ϕ_{AI} in the i th cluster normalized by its central angular path's power is given by:

$$AOA_I(\phi_{ik}) = e^{-|\phi_{ik}|/\phi_{AI}} \quad (0 \leq |\phi_{ik}| \leq 180) \quad (77)$$

where ϕ_{AI} denotes the average arrival angle in the cluster. $\phi_{AI} = 180^\circ$ is a typical value.

1.4.2 Generation of reduced variability models based on TSP model

1.4.2.1 NLoS scenario for base coverage macrocell

The reduced variability model is created by setting its key parameters. Each channel can be realized by the following procedure:

Step 1: Set test environments and key parameters

Set the following parameters.

a) *Frequency conditions*

f_c : carrier frequency (MHz)

λ : wavelength of carrier frequency (m) (= $300/f_c$)

B : bandwidth or chip rate (MHz).

b) *City structures*

$\langle H \rangle$: average building height (m). (Bad-urban: 30 m, Urban: 20 m, Suburban: 10 m, Residential: 8 m, Rural: 5 m, etc.)

W : road width (m) (Bad-urban: 20 m, Urban: 20 m, Suburban: 20 m, Residential: 20 m, Rural: 20 m, etc.).

c) *Cell conditions*

h_b : BS antenna height (m).

h_m : UT antenna height (m)

d : distance from the BS (m).

Step 2: Set the simulation conditions

N_{path} : number of clusters for NLoS

N_{path}^S : number of clusters for LoS

ΔL_{th} : level difference between the peak path's power and cut off power in NLoS scenario (dB)

ΔL_{th}^S : level difference between the peak path's power and cut off power for scattering clusters in LoS scenario (dB).

Step 3: Generation of long-term TSP

Step 3.1: Generation of delay time

a) *Calculation of maximum delay time*

Convert excess distance l (m) into excess delay time τ (μ s) by equation (78):

$$\tau = l / (300 / f_c) \quad (\mu s) \quad (78)$$

The maximum delay time can be calculated by considering ΔL_{th} as follows:

$$PDP_L(\tau_{LMax}, d) = -\Delta L_{th} \quad (\Delta L_{th} \geq 0) \quad (79)$$

Solving the above equation yields the maximum delay time τ_{LMax} .

b) *Dynamic delay time of each cluster*

The delay time interval $\Delta\tau_L$ is calculated as follows:

$$\Delta\tau_L = \tau_{LMax} / (N_{path} - 1) \quad (80)$$

The dynamic delay time is generated by using a random number:

$$\tau_L(i) = \begin{cases} 0 & (i = 0) \\ i\Delta\tau_L + \Delta\tau_L(\text{Random}[0,1] - 1/2) & (i = 1, 2, \dots, N_{path} - 1) \end{cases} \quad (81)$$

where $\text{Random}[0,1]$ denotes a random value with uniform distribution between 0 and 1.

c) *Fixed delay time of each cluster*

Instead of the dynamic delay time, fixed delay time $\tau_L(i)$ is given as follows. Table A1-23 shows the normalized fixed delay time $\tau_L^N(i)$. When the number of clusters and the maximum delay time are given, the fixed delay time $\tau_L(i)$ is calculated by using Table A1-23 by:

$$\tau_L(i) = \tau_{LMax} / \left(\tau_L^N(i) / \tau_L^N(N_{path} - 1) \right) \quad (i = 0, 1, 2, \dots, N_{path} - 1) \quad (82)$$

where $\tau_{LMax} / \left(\tau_L^N(N_{path} - 1) \right)$ represents the scaling factor.

TABLE A1-23

Parameter sets of $\tau_L(i)$ and X_i^N

a) For the case of $N_{path} = 20$

Index number i	Normalized delay time $\tau_L(i)$	Normalized short term variation X_i^N with STD of 1 (dB)			
		$X_i^{N(1)}$	$X_i^{N(2)}$	$X_i^{N(3)}$	$X_i^{N(4)}$
1	0.0000	0.24064	0.18409	0.26383	0.74152
2	0.047	-0.69579	-0.12405	1.9716	0.83339
3	0.097	0.37050	-0.0077560	-0.40653	-2.5006
4	0.129	-0.89163	-0.26097	0.63798	-1.6534
5	0.215	-0.82499	0.92161	0.16647	0.52677
6	0.253	0.54805	0.35463	1.3216	1.2068
7	0.298	-1.6740	-0.13014	-0.46038	-0.54795
8	0.343	-1.7426	0.44910	1.0759	-0.26516
9	0.397	0.96705	-0.021601	1.3793	1.7035
10	0.452	-0.57140	-2.6355	-0.30171	0.53209
11	0.507	0.61279	0.16136	-0.33711	-0.75249
12	0.534	0.042949	-0.77649	-1.6624	-0.11695
13	0.615	-0.59649	2.0748	0.31816	0.74633
14	0.645	1.9803	0.76392	-0.91974	-1.6244
15	0.692	-0.13612	-1.3529	0.56334	0.22220
16	0.727	-0.58639	0.50109	-0.99308	0.15922
17	0.817	-0.19525	0.12992	0.49671	0.65203
18	0.861	-1.6267	0.77200	-1.0752	0.16436
19	0.913	1.6513	-1.7319	-1.9479	-0.31058
20	0.956	-0.12564	0.72884	-0.090964	0.28327

TABLE A1-23 (end)

b) For the case of $N_{path} = 10$

Index number i	Normalized delay time $\tau_L(i)$	Normalized short term variation X_i^N with STD of 1 (dB)			
		$X_i^{N(1)}$	$X_i^{N(2)}$	$X_i^{N(3)}$	$X_i^{N(4)}$
1	0.0000	1.1458	1.2001	1.7690	0.48474
2	0.094923	0.75311	0.53053	0.060735	0.43398
3	0.19599	-0.70881	1.0645	-1.9474	0.058202
4	0.25979	1.6582	0.56882	0.20572	-2.0529
5	0.43136	-1.1183	-1.4115	-0.66017	-0.35828
6	0.50651	-0.78058	0.052757	-0.49775	0.48382
7	0.59619	-1.4302	-0.86393	1.2526	-1.0723
8	0.68790	0.91257	-0.66617	-0.33581	-0.37723
9	0.79581	-0.35092	1.0897	0.64893	1.8421
10	0.90483	-0.080880	-1.5649	-0.49588	0.55783

Step 3.2: Generation of relative power (without considering short-term variation)

The delay profile is normalized by the first cluster's power as follows:

$$PDP_L(i, d) \equiv PDP_L(\tau_L(i), d) \quad \text{dB} \quad (83)$$

Set the delay profile normalized by all clusters' power as 1 (= 0 dB):

$$PDP_{LN}(i, d) = PDP_L(i, d) - PDP_{Lnorm}(d) \quad \text{dB} \quad (84)$$

where $PDP_{Lnorm}(d)$ represents all clusters' power as follows:

$$PDP_{Lnorm}(d) = 10 \log \left(\sum_{i=0}^{N_{path}-1} 10^{PDP_L(i, d)/10} \right) \quad \text{dB} \quad (85)$$

Step 3.3: Generation of departure angle

Set the departure angle of the i th cluster as follows:

$$\theta_{LD}(i, d) = (-1)^i a (PDP_L(i\Delta\tau_L, d))^{-1/\beta} - 1 \quad (i = 0, 1, 2, \dots, N_{path} - 1) \text{ degrees} \quad (86)$$

Step 3.4: Generation of arrival angle

Set the arrival angle of the i th cluster as follows:

$$\theta_{LA}(i, d) = (-1)^i \cos^{-1} \left(\frac{(2d^2 + 2di\Delta\tau_L + (i\Delta\tau_L)^2) \cos \theta_{LD}(i) - 2d(d + i\Delta\tau_L)}{2d^2 + 2di\Delta\tau_L + (i\Delta\tau_L)^2 - 2d(d + i\Delta\tau_L) \cos \theta_{LD}(i)} \right) \text{ degrees} \quad (87)$$

Steps 3.1 to 3.4 yield the delay time, departure angle, arrival angle, and normalized relative power for each cluster.

Step 4: Generation of short-term variation

a) *Dynamic short term variation*

The dynamic short term variation of each cluster x_i follows an independent log-normal distribution as equation (88):

$$G(X_i) = e^{-X_i^2/2\sigma_s^2} / \sqrt{2\pi}\sigma_s \quad (88)$$

where σ_s represents the standard deviation of short term variation.

b) *Fixed short term variation*

Instead of the dynamic short-term variation, fixed short term variation X_i can be easily obtained based on Table A1-23 by using the following equation:

$$X_i = \sigma_s X_i^N \quad (i = 0, 1, 2, \dots, N_{path} - 1) \quad (89)$$

where X_i^N represents a normalized short term variation, with standard deviation of 1, obtained from Table A1-23. A typical standard deviation value for σ_s is 4.5 dB for macro-cell.

Step 5: Generation of relative power considering short-term variation

Instead of using the relative power without short-term variation as per Step 3.2, the relative power with short-term variation $PDP_{L\&S}(i, d)$ can be obtained as follows:

$$PDP_{L\&S}(i, d) = PDP_L(i, d) + X_i \quad \text{dB} \quad (90)$$

1.4.2.2 LoS scenario for base coverage macro-cell

The LoS environment consists of direct clusters and scattering clusters. The time and spatial characteristics of scattering clusters are completely the same as those of NLoS.

Channel realizations for LoS are achieved by the following procedure:

Step 1 and Step 2: Set the conditions as per the NLoS case.

Step 3: Generation of direct clusters.

Direct clusters consist of three direct clusters, $P_{D,i}(i = 0, 1, 2)$. Generate delay time $\tau_{D,i}(i, d)$, arrival angle $\theta_{DA,i}(i, d)$, departure angle $\theta_{DD,i}(i, d)$ and relative power $PDP_{D,i}(i, d)$ normalized against the first cluster's power as follows:

a) $\tau_{D,i}(i, d)$

$$\tau_{D,0}(0, d) = 0, \tau_{D,1}(1, d) = W^2 / (300d), \tau_{D,2}(2, d) = 3W^2 / (300d) \quad (\mu\text{s}) \quad (91)$$

b) $\theta_{DA,i}(i, d)$

$$\theta_{DA,0}(0, d) = 0, \theta_{DA,1}(1, d) = 2W / d \cdot (180 / \pi), \theta_{DA,2}(2, d) = -2W / d \cdot (180 / \pi) \quad \text{degrees} \quad (92)$$

c) $\theta_{DD,i}(i, d)$

$$\theta_{DD,0}(0, d) = 0, \theta_{DD,1}(1, d) = W / d \cdot (180 / \pi), \theta_{DD,2}(2, d) = 2W / d \cdot (180 / \pi) \quad \text{degrees} \quad (93)$$

d) $PDP_{D,i}(i, d)$

$$PDP_{D,0}(0, d) = 1, PDP_{D,1}(1, d) = 0.3, PDP_{D,2}(2, d) = 0.1 \quad (94)$$

Step 4: Generation of scattering clusters

Step 4.1: Generation of delay time for scattering clusters

Scattering clusters consist of $(N_{path}^S - 3)$ clusters.

a) The PDP for scattering clusters is given by:

$$PDP_{L,scatter}(k, d) = PDP_L(k\Delta\tau_L, d) - 12 \quad \text{dB} \quad (95)$$

b) Calculation of maximum delay time

The maximum delay time is calculated to satisfy the following equation involving a threshold level ΔL_{th}^S :

$$PDP_L(\tau_{LMax}, d) = -\Delta L_{th}^S \quad (\Delta L_{th}^S \geq 0) \quad (96)$$

Solving the above equation yields the maximum delay time τ_{LMax}^S . ΔL_{th}^S is generally given by $\Delta L_{th}^S = \Delta L_{th} - 12$ (dB).

Step 4.2: Generation of delay time, relative power (without considering short-term variation), departure angle, arrival angle, and relative power considering short-term variation for scattering clusters.

This step is completely the same as Step 3 to Step 5 in the NLoS case.

Step 5: Generation of the power delay profile considering the direct and scattering clusters

Step 5.1: Generation of relative power (without considering short-term variation)

a) *Dynamic delay time of each cluster*

The delay time interval $\Delta\tau_L$ is calculated as follows:

$$\Delta\tau_L = \tau_{LMax} / (N_{path}^S - 3) \quad (97)$$

The dynamic delay time is generated by using a random number:

$$\tau_{LLOS}(i) = \begin{cases} \tau_{D,i}(i, d) & (i = 0, 1, 2) \\ (i-2)\Delta\tau_L + \Delta\tau_L(\text{Random}[0,1] - 1/2) & (i = 3, \dots, N_{path}^S - 1) \end{cases} \quad (98)$$

Where $\text{Random}[0,1]$ denotes a random value with uniform distribution between 0 and 1.

b) *Fixed delay time of each cluster*

Instead of the dynamic delay time, fixed delay time $\tau_L(i)$ is given as follows. Table A1-23 shows the normalized fixed delay time $\tau_L^N(i)$. When the number of clusters and the maximum delay time are given, the fixed delay time $\tau_L(i)$ is calculated by using Table A1-23 as follows:

$$\tau_{LLOS}(i) = \tau_{LLOS}^N(i-2) \left(\frac{\tau_{LLOSMax}^N}{\tau_{LLOS}^N (N_{path}^S - 3)} \right) \quad (i = 3, \dots, N_{path}^S - 1) \quad (99)$$

where $\tau_{LLOSMax}^N / (\tau_{LLOS}^N (N_{path}^S - 3))$ represents the scaling factor.

Step 5.2: Generation of relative power (without considering short-term variation).

The delay profile considering the direct clusters and scattering clusters is given by:

$$PDP_{LLOS}(i, d) = \begin{cases} 10 \log \left(PDP_{D,i}(i, d) + 10^{PDP_{L,scatter}(0,d)/10} \right) & (0 \leq i \leq 2) \\ PDP_{L,scatter}(i-2, d) & (3 \leq i \leq N_{path}^S - 1) \end{cases} \quad \text{dB} \quad (100)$$

Set the delay profile normalized by the first cluster's power as follows:

$$PDP_{LLOS^N}(i, d) = PDP_{LLOS}(i, d) - PDP_{LLOS}(0, d) \quad \text{dB} \quad (101)$$

Step 5.3: Generation of departure angle

Set the departure angle of the i th cluster as follows:

$$\theta_{LDLOS}(i, d) = \begin{cases} \theta_{DD,i}(i, d) & (i = 0, 1, 2) \\ (-1)^{(i-2)} \alpha(PDP_L((i-2)\Delta\tau_L, d)^{-1/\beta} - 1) & (i = 3, \dots, N_{path}^S - 1) \end{cases} \text{degrees} \quad (102)$$

Step 5.4: Generation of arrival angle

Set the arrival angle of the i th cluster as follows:

$$\theta_{LALOS}(i, d) = \begin{cases} \theta_{DA,i}(i, d) & (i = 0, 1, 2) \\ (-1)^{i-2} \cos^{-1} \left(\frac{(2d^2 + 2d(i-2)\Delta\tau_L + ((i-2)\Delta\tau_L)^2) \cos \theta_{LD}((i-2)) - 2d(d + (i-2)\Delta\tau_L)}{2d^2 + 2d(i-2)\Delta\tau_L + ((i-2)\Delta\tau_L)^2 - 2d(d + (i-2)\Delta\tau_L) \cos \theta_{LD}((i-2))} \right) & (i = 3, \dots, N_{path}^S - 1) \end{cases} \text{degrees} \quad (103)$$

Steps 5.1 to 5.4 yield the delay time, departure angle, arrival angle, and normalized relative power for each cluster.

1.4.3 K -factor

In the NLoS case, the K -factor is basically $0 (= -\infty \text{ dB})$. In the LoS case, the K -factor of the direct cluster is determined by the ratio of the direct cluster's power to the first scattering cluster's power. On the other hand, the K -factor of the other scattering clusters is basically $0 (= -\infty \text{ dB})$.

1.4.4 Cross polarization

a) VV, VH, HH and HV

$PDP_{L\&S}^{VV}(i, d)$, $PDP_{L\&S}^{VH}(i, d)$, $PDP_{L\&S}^{HH}(i, d)$ and $PDP_{L\&S}^{HV}(i, d)$ express delay profiles with short-term variation due to vertical-to-vertical (VV), vertical-to-horizontal (VH), horizontal-to-horizontal (HH) and horizontal-to-vertical (HV) polarization, respectively as follows:

$$PDP_{L\&S}^{VV}(i, d) = PDP_L(i, d) + X_i^{(1)} \quad \text{dB} \quad (104a)$$

$$PDP_{L\&S}^{VH}(i, d) = PDP_L(i, d) - XPD_L + X_i^{(2)} \quad \text{dB} \quad (104b)$$

$$PDP_{L\&S}^{HH}(i, d) = PDP_L(i, d) + X_i^{(3)} \quad \text{dB} \quad (104c)$$

$$PDP_{L\&S}^{HV}(i, d) = PDP_L(i, d) - XPD_L + X_i^{(4)} \quad \text{dB} \quad (104d)$$

where $X_i^{(1)}$, $X_i^{(2)}$, $X_i^{(3)}$ and $X_i^{(4)}$ are independent random variables following log-normal distributions with standard deviation of σ_s . If these values are required to be fixed, these values can be generated by using the normalized variations $X_i^{N(k)}$ in Table A1-23 and the relation $X_i^{(k)} = \sigma_s X_i^{N(k)}$ ($k = 1, 2, \dots, 4$).

1.4.5 Generation of small scale parameters in clusters

Instantaneous time-spatial profiles can be generated by using small-scale parameters.

This process generation is applied for all NLoS clusters and all LoS scattering clusters.

Step 1: Simulation condition

N_p : number of paths in cluster.

Step 2: Generation of delay time

The delay time interval $\Delta\tau_I$ and delay time τ_I normalized by the first path's delay time in a cluster are calculated respectively as follows:

$$\Delta\tau_I = \tau_{I_{max}} / (N_p - 1) \text{ } \mu\text{s} \quad (105)$$

$$\tau_I(k) = k\Delta\tau_I \quad (k = 0, 1, 2, \dots, N_p - 1) \text{ } \mu\text{s} \quad (106)$$

Here $\tau_{I_{max}}$ denotes the maximum delay time. It is typically 0.1 μs and 0 μs in the simplest case. Delay time $\tau_I(k)$ is recalculated at a time interval of $\Delta\tau_I$.

Step 3: Generation of relative power

The delay profile normalized by the first path's power in a cluster is expressed as:

$$PDP_I(k) = 10 \log(e^{-\tau_I(k)/\tau_{I_{av}}}) = 10 \log(e^{-k\Delta\tau_I/\tau_{I_{av}}}) \text{ dB} \quad (107)$$

where $\tau_{I_{av}}$ is the average delay time of each cluster. $\tau_{I_{av}}$ is typically 0.1 μs and 0 μs in the simplest case. Set the delay profile normalized by all paths' power in a cluster as follows:

$$PDP_{IN}(k) = PDP_I(k) - PDP_{Inorm} \text{ dB} \quad (108)$$

where PDP_{Inorm} represents all paths' power in a cluster according to:

$$PDP_{Inorm} = 10 \log \left(\sum_{k=0}^{N_p-1} 10^{PDP_I(k)/10} \right) \text{ dB} \quad (109)$$

Step 4: Generation of arrival angle

The arrival angle interval $\Delta\phi_{IA}$ is set as follows:

$$\Delta\phi_{IA} = 180 / N_p \text{ degrees} \quad (110)$$

Set the arrival angle of the k th path in a cluster as follows:

$$\phi_{IA}(k) = (-1)^k k\Delta\phi_{IA} \text{ (deg.)} \quad (k = 0, 1, \dots, N_p - 1) \quad (111)$$

The arrival angle $\phi_{IA}(k)$ is calculated using the angular interval $\Delta\phi_{IA}$.

Step 5: Generation of departure angle

The departure angle interval $\Delta\phi_{ID}$ is set as follows:

$$\Delta\phi_{ID}(i) = \frac{\phi_{ID}(i)\Delta\tau_I}{\tau_{I_{av}}} \text{ degrees} \quad (112)$$

where:

$$\phi_{ID}(i) = \frac{60}{(d + i \cdot (300/B))} \cdot \frac{180}{\pi} \text{ degrees} \quad (113)$$

Set the departure angle in a cluster according to:

$$\phi_{ID}(i, k) = (-1)^k k\Delta\phi_{ID}(i) \text{ (deg.)} \quad (k = 0, 1, 2, \dots, N_p - 1) \quad (114)$$

Steps 1 to 3 yield the delay time, departure angle, arrival angle, and normalized relative power of paths in each cluster. Note that when $\tau_{I_{max}}$ is set to 0 μs , the fading model in the clusters becomes the well-known Clark model.

1.4.6 Typical values of parameters

1.4.6.1 Large scale parameters

The typical number of clusters for the reduced variability model based on the TSP model is shown in Table A1-24 for NLoS scenarios and Table A1-25 for LoS scenarios.

TABLE A1-24
NLoS scenarios (typical)

City structure		Number of clusters N_{path} (typical)	Level difference of clusters ΔL_{th} (dB) (typical)
(*)	Dense urban	20	25
UMa	Urban	20	
SMa	Suburban	20	
(*)	Residential	10	
RMa	Rural	10	

TABLE A1-25
LoS scenarios (typical)

City structure		Number of direct clusters (typical)	Number of scattering clusters N_{path} (typical)	Level difference of scattering clusters ΔL_{th}^S (dB) (typical)
(*)	Dense urban	3	10	13
UMa	Urban		10	
SMa	Suburban		10	
(*)	Residential		10	
RMa	Rural		10	

1.4.6.2 Small scale parameters

The typical number of rays in a cluster with the reduced variability model is shown in Table A1-26. There are two parameter sets: The first one is for the realistic model and the second for the classical model. The classical model is realized by setting τ_{Imax} to 0 μs (known as Clark's model). Note that the received level depends on just the UT moving speed, not the UT moving direction in the classical model.

TABLE A1-26

Small scale parameters

Parameter	Realistic model (typical)	Classical model (typical)
N_p	20	20
τ_{lmax}	0.1 μ s ($l_{lmax} = 30$ m)	0 μ s ($\tau_l(k) \equiv 0, \Delta\phi_{lD}(i) \equiv 0, PDP_l(k) \equiv 0$ dB)
Noting		Highly-reproducible and convenient model

1.4.6.3 Identification of the model

In order to clarify the model generated by the extension module, the generated model has to be identified. For example, when the reduced variability model in the extension module is used, the applied model can be identified by describing it as “Extension module (TSP model)- reduced variability model- NLoS (typical)- Classical model (typical)”.

References

- DONG, W., ZHANG, J., GAO, X., ZHANG, P. and WU, Y. [2007] Cluster Identification and Properties of Outdoor Wideband MIMO Channel. Vehicular Technology Conference, 2007. VTC-2007 Fall. 2007 IEEE 66th, Sept. 30 2007-Oct. 3 2007, p. 829 – 833.
- FUJII, T. [2003] Path-loss prediction formula in mobile communication -an expansion of “SAKAGAMI” path-loss prediction formula-. *Trans. IEICE*, Japan, J86-B, 10, p. 2264-2267.
- FUJII, T. [2004] Delay profile modelling for wideband mobile propagation. Proc. of IEEE 2004 VTC Fall F.
- GAO, X., ZHANG, J., LIU, G., XU, D., ZHANG, P., LU Y. and DONG, W. [December 2007] Large-Scale Characteristics of 5.25 GHz Based on Wideband MIMO Channel Measurements. *Ant. and Wireless Propag. Lett.*, Vol.6, p. 263-266.
- KERMOAL, J. P., SCHUMACHER, L., PEDERSEN, K. L., MOGENSEN, P. E. and FREDERIKSEN, F. [2002] A stochastic MIMO radio channel model with experimental validation. *IEEE J. Select. Areas in Comm.*, Vol. 20, 6, p. 1211-1226.
- LU, Y., ZHANG, J., GAO, X., ZHANG, P. and WU, Y. [2007] Outdoor-Indoor Propagation Characteristics of Peer-to-Peer System at 5.25 GHz. Vehicular Technology Conference, 2007. VTC-2007 Fall. 2007 IEEE 66th, Sept. 30 2007-Oct. 3 2007, p. 869-873.
- OHTA, Y. and FUJII, T. [2006] Delay Spread Prediction for wideband mobile propagation. Proc. of IEEE 2006 VTC, Montreal.
- OKAMOTO, H. and ICHITSUBO, S. [March 2005] Investigations of outdoor-to-indoor propagation loss on 800MHz-8GHz at urban area. Proc. The 2005 IEICE General Conference, Japan, p. S23-S24, (in Japanese).
- OMOTE, H. and FUJII, T. [2007] Empirical arrival angle profile prediction formula for mobile communication system. Proc. of IEEE 2007 VTC Spring, Dublin.
- SMITH, P. J. and SHAFI, M. [June 2004] The impact of complexity in MIMO channel models. Proc. of IEEE International Conference on Communications (ICC '04), Vol. 5, p. 2924-2928, Paris, France.
- XU, D., ZHANG, J., GAO, X., ZHANG, P. and WU, Y. [2007] Indoor Office Propagation Measurements and Path Loss Models at 5.25 GHz. Vehicular Technology Conference, 2007. VTC-2007 Fall. 2007 IEEE 66th, Sept. 30 2007-Oct. 3 2007, p. 844-848.

- ZHANG, J., GAO, X., ZHANG, P. and YIN, X. [3-7 September 2007] Propagation Characteristics of Wideband MIMO Channel in Hotspot Areas at 5.25 GHz. Personal, Indoor and Mobile Radio Communications, 2007. PIMRC 2007. IEEE 18th International Symposium on September.
- ZHANG, J., DONG, D., LIANG, Y., NIE, X., GAO, X., ZHANG, Y., HUANG, CH. and LIU, G. [2008] Propagation characteristics of wideband MIMO channel in urban micro- and macrocell. IEEE PIMRC 2008, Invited paper.

Bibliography

- GUDMUNDSON, M. [November 1991] Correlation Model for Shadow Fading in Mobile Radio Systems. *Electron. Lett.*, Vol. 27, 23, p. 2145-2146).
- FORTUNY-GUASCH J. *et al.* [October 2006] UWB screening attenuation measurements of cars study by IPSC of the JRC and ETSI TG31C on the measurement of the screening attenuation of cars in the frequency range between 0.85 GHz and 11 GHz. IPSC, Sensors Radar Technologies and Cyber Security Unit, European Commission Joint Research Centre. EUR 22532 EN.
- 3GPP TSG-RAN1#48, R1-070674, LTE physical layer framework for performance verification, Orange, China Mobile, KPN, NTT DoCoMo, Sprint, T-Mobile, Vodafone, Telecom Italia.
- NGMN White paper [December 2007] Next Generation Mobile Networks Radio Access Performance Evaluation Methodology.
- 3GPP-SCM [September 2003] Spatial channel model for multiple input multiple output (MIMO) simulations, TR 25.996 v.6.1.0.

ITU-R texts

- Recommendation ITU-R P.679-1.
- Proposed New Test Environments and Channel Models of Preliminary Draft New Report M.[IMT.EVAL], Doc. 5D/62, January 2008, Geneva, Switzerland.
- Channel Models for Evaluation of Air Interface Proposals for IMT-Advanced, Doc. 5D/68, January 2008, Geneva, Switzerland.
- Proposed Propagation Models for Evaluation Radio Transmission Technologies in IMT-Advanced, Doc. 5D/88, January 2008, Geneva, Switzerland.

Annex 2

Traffic models

There are two types of traffic models which should be used for evaluation of proposed IMT-Advanced RIT or SRITs:

- Full buffer traffic model, and
- VoIP traffic model.

1 Full buffer traffic model

In the full buffer traffic model (sometimes referred to as a full queue model) there is an infinite amount of data bits awaiting transmission in the transmit buffer associated with each data source. For uplink traffic the transmit buffers exist in the user terminal while for downlink traffic the transmit buffers exist in the network infrastructure, e.g., in the base station.

2 VoIP traffic model

Table A2-1 provides the relevant parameters of the VoIP traffic that should be used for the simulations. The details of the corresponding traffic model are described below:

TABLE A2-1

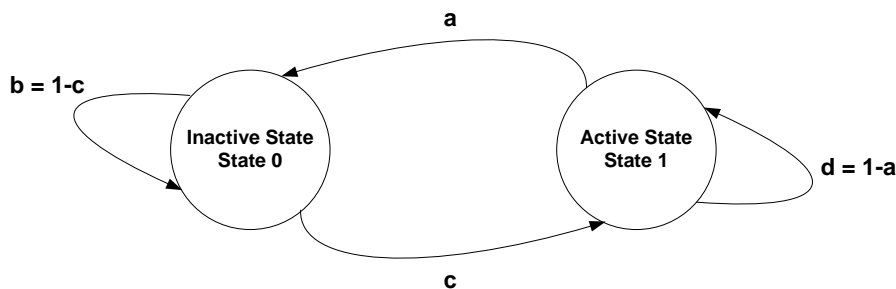
Parameter	Characterization
Codec	Source rate 12.2 kbit/s
Encoder frame length	20 ms
Voice activity factor (VAF)	50% ($c = 0.01$, $d = 0.99$)
SID payload	Modelled 15 bytes (5 bytes + header) SID packet every 160 ms during silence
Protocol overhead with compressed header	10 bit + padding (RTP-pre-header) 4 bytes (RTP/UDP/IP) 2 bytes (RLC/security) 16 bits (CRC)

2.1 Detailed description of the VoIP traffic model

a) Basic model

Consider the simple 2-state voice activity model shown in Fig. 14.

FIGURE 14
2-state voice activity model



In the model, the probability of transitioning from state 1 (the active speech state) to state 0 (the inactive or silent state) while in state 1 is equal to a , while the probability of transitioning from state 0 to state 1 while in state 0 is c . The model is assumed updated at the speech encoder frame rate $R = 1/T$, where T is the encoder frame duration (typically, 20 ms).

b) Model statistics

The steady-state equilibrium of the model requires that:

$$\begin{aligned}
 P_0 &= \frac{a}{a + c} \\
 P_1 &= \frac{c}{a + c}
 \end{aligned}
 \tag{115}$$

where P_0 and P_1 are respectively the probability of being in state 0 and state 1.

The voice activity factor (VAF) λ is given by:

$$\lambda = P_1 = \frac{c}{a+c} \quad (116)$$

A talk-spurt is defined as the time period τ_{TS} between entering the active state (state 1) and leaving the active state. The probability that a talk spurt has duration n speech frames is given by:

$$P_{\tau_{TS}=n} \triangleq P_{TS}(n) = a(1-a)^{n-1} \quad n=1,2,\dots \quad (117)$$

Correspondingly, the probability that a silence period has duration n speech frames is given by:

$$P_{\tau_{SP}=n} \triangleq P_{SP}(n) = c(1-c)^{n-1} \quad n=1,2,\dots \quad (118)$$

The mean talk spurt duration μ_{TS} (in speech frames) is given by:

$$\mu_{TS} = E[\tau_{TS}] = \frac{1}{a} \quad (119)$$

while the mean silence period duration μ_{SP} (in speech frames) is given by:

$$\mu_{SP} = E[\tau_{SP}] = \frac{1}{c} \quad (120)$$

The distribution of the time period τ_{AE} (in speech frames) between successive active state entries is the convolution of the distributions of τ_{SP} and τ_{TS} . This is given by:

$$P_{\tau_{AE}=n} \triangleq P_{AE}(n) = \frac{c}{c-a} a(1-a)^{n-1} + \frac{a}{a-c} c(1-c)^{n-1} \quad n=1,2,\dots \quad (121)$$

Note that τ_{AE} can be used as a crude guide to the time between MAC layer resource reservations, provided a single reservation is made per user per talk-spurt. Note that in practice, very small values of τ_{AE} might not lead to a separate reservation request, but equation (121) still offers some potentially useful guidance.

Since the state transitions from state 1 to state 0 and vice versa are independent, the mean time μ_{AE} between active state entries is given simply by the sum of the mean time in each state. That is:

$$\mu_{AE} = \mu_{TS} + \mu_{SP} \quad (122)$$

Accordingly, the mean rate of arrival \bar{R}_{AE} of transitions into the active state is given by:

$$\bar{R}_{AE} = \frac{1}{\mu_{AE}} \quad (123)$$